FLASHOVER PREVENTION ON POLYSTYRENE HIGH VOLTAGE INSULATORS IN A VACUUM

A Thesis
Presented to
The Faculty of the Graduate School
at the University of Missouri-Columbia

In Partial Fulfillment
of the Requirements of the Degree

Master of Science

by
ANDREW BENWELL

Dr. Scott Kovaleski, Thesis Supervisor

DECEMBER 2007

The undersigned, appointed by the dean of the Graduate School, have examined the thesis entitled

FLASHOVER PREVENTION ON POLYSTYRENE
HIGH VOLTAGE INSULATORS IN A VACUUM

presented by Andrew Benwell,

a candidate for the degree of master of science,

and hereby certify that, in their opinion, it is worthy of acceptance.

Professor Scott Kovaleski

Professor John Gahl

Professor Mark Prelas

Acknowledgements

I would first like to extend special thanks to my advisor, Dr. Scott Kovaleski for his guidance and the occasional swift kick, encouraging me to finish.

I would like to thank Dr. John Gahl for his enthusiasm toward research which encouraged me to pursue a graduate degree.

I would like to thank Dr. Ken Struve at Sandia National Laboratories for his interest in performing flashover research at the University of Missouri.

I would like to extend special thanks to Dr. Keith Lechien and PhD Candidate Mark Kemp for their willingness to discuss and brainstorm and to teach me with their graduate research experience.

I would like to thank the many undergraduates who worked in and were associated with the MUTTS facility. I would like to extend special thanks to Bill Baldridge, Tim Evans, Brian Hutsel, Mike Hutsel, Brandon Morgen, Tyler Nichols, and Jim Vangordon for all of the time and effort that made my research possible.

I would like to thank my parents for their emphasis on education and their encouragement towards pursuing a graduate degree.

I especially thank my wife, Risa, for her patience and support while I have pursued my degree, and for understanding the long, irregular hours.

Table of Contents

List of Figures

List of Tables

Introduction

A. Flashover in pulsed power systems

i. Insulator Stacks

Plastic insulators are frequently used to separate high voltage conductors in large pulsed power machines. At interfaces where power flow must move into a vacuum region, plastic insulators are used to create a barrier at the vacuum boundary [1]. Insulator stacks are insulating barriers that are commonly used at water-vacuum interfaces, where energy flowing through water transmission lines is transferred to vacuum transmission lines for use in high energy density experiments.

At these boundaries, insulator stacks are used for separating multiple anode-cathode pairs. For many reasons, these boundaries can also result in a limiting region

where flashover is most likely to occur if the insulator is stressed beyond a tolerable amount [2;3]. The design of insulator filled regions needs to be very thoroughly considered so that the insulator performs the job of separating conductors while not actually resulting in flashover.

Under currently used technology, many pulsed power vacuum insulator stacks are considered very large in size due to the electrical stress limits of an insulator. The Z-machine vacuum barrier takes the form of plastic rings, approximately 11-ft. in diameter, stacked one on top of the other forming an insulator stack [3]. It is desirable to minimize the size of the insulator to reduce their expense and for other technical reasons [1]. It is therefore necessary to increase the electrical stress limit that the insulator is able to withstand so that the physical size can be reduced. This may be accomplished in different ways including electrical shielding, and insulator geometry. However, new techniques also need to be developed in order to further increase the stress limit of electrical insulators [4].

A typical insulator stack, for a large pulsed power driver, includes multiple pieces of insulating material placed between metal conductors [3]. The metal spacers between the plastic pieces help to evenly distribute the electrical field across the surface of the insulator. Figure 1 shows a typical insulator stack. The insulator surface near vacuum has been demonstrated to be least likely to flash with the use of a +45 degree angle [5-7]. This means that the insulator extends further along the cathode conductor forming a 45 degree angle with the normal of the conductor as shown in Figure 2.

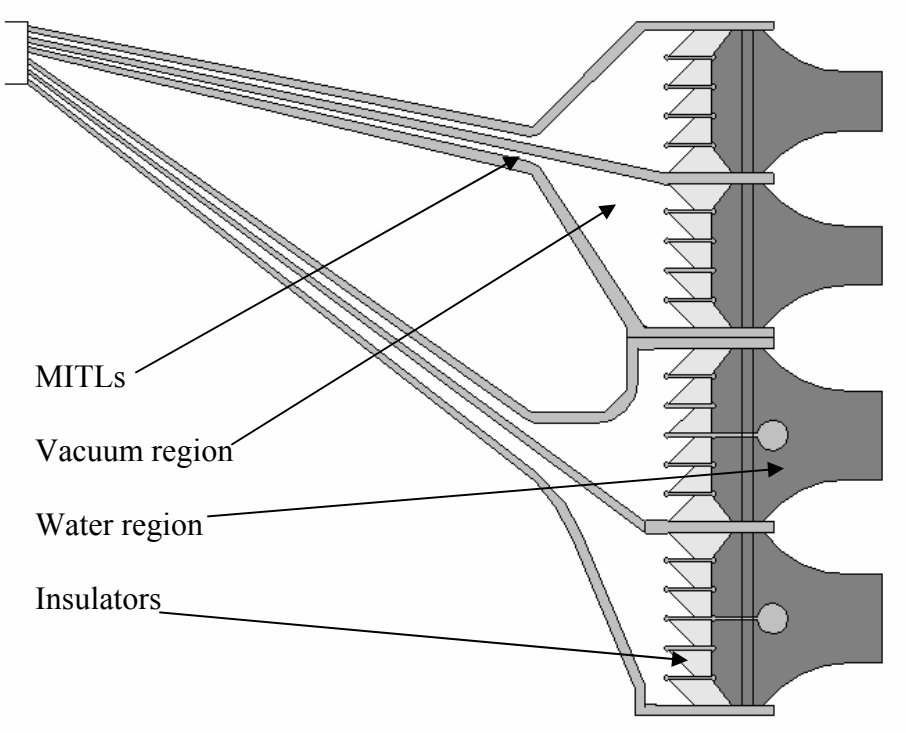

Figure 1: Example Insulator Stack and MITL from Z, symmetrical about the left side [8].

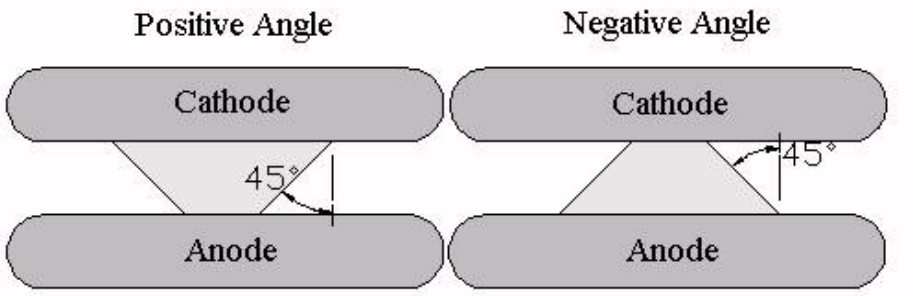

Figure 2: Positive and negative angles formed between insulator and conductors[6].

A +45 degree insulator angle using polystyrene has been shown to increase the vacuum flashover voltage across a similar gap by a factor of 2 or more [6;7]. Geometric modifications to zero degree insulating surfaces, such as changing the surface angle and adding conductive field shapers are widely used methods to try to increase insulator

flashover voltage [5;9].

ii. Future Machine Requirements

Requirements for future pulsed power machines indicate that the maximum electrical stress level of an insulator stack must increase. The insulator stack of the Z machine operates under a peak electric field of 105 kV/cm. The Z refurbishment project plans to increase the stress of the insulators up to 140 kV/cm [4]. As the stress level of a typical insulator increases, the probability of flashover also increases [10].

The maximum stress level is a limiting factor in the design of insulator stacks. The size of similar pulsed power machines can be reduced if the insulating barrier can operate at higher electrical stresses without flashover occurring [1]. Smaller insulator stacks will lead to lower inductance and reduced cost for these components [3]. Different techniques to increase the operation level of insulator stacks are being examined.

Two techniques that may accomplish this feat are reduction of electric field near the anode and cathode triple points [1], and use of a self-generated magnetic field to prevent the flashover process from initiating at high voltages [11].

iii. Triple Point Shielding

The use of an insulator stack results in a region in which the power must flow past a transition from plastic as the dielectric to vacuum as the dielectric. In this region, the change of relative dielectric strength from inside the insulator to inside the vacuum results in an uneven electric field across the insulator surface [12]. Non-uniform distributions of the electric field can result in regions of high electric field on the insulator surface near the triple point. For this reason it is sometimes beneficial to redistribute the electrical field across the insulator with the use of field shaping

conductors [9].

Figure 3 and Figure 4 are electrostatic field simulations showing the redistribution of an electric field along an insulating surface [13]. The regions marked “Anode” and “Cathode” are simulated as perfect conductors with an applied voltage. The trapezoid shape in between the conductors is an insulator with a relative dielectric strength of 2.1, and all other space is a vacuum.

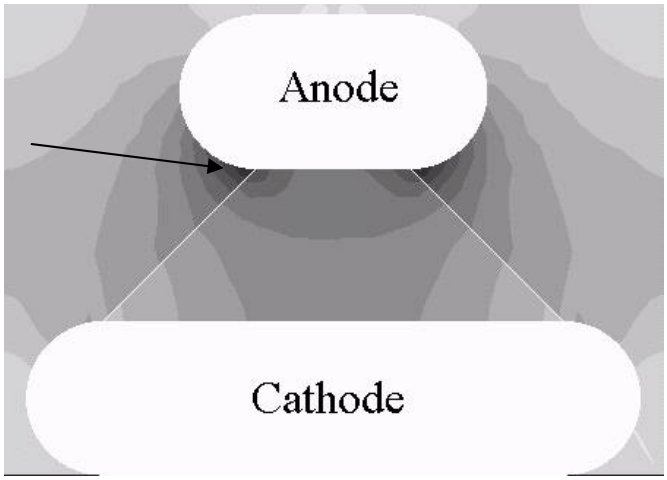

Figure 3: Electric field for an unshaped field geometry. The arrow is pointing to a region of high electric field.

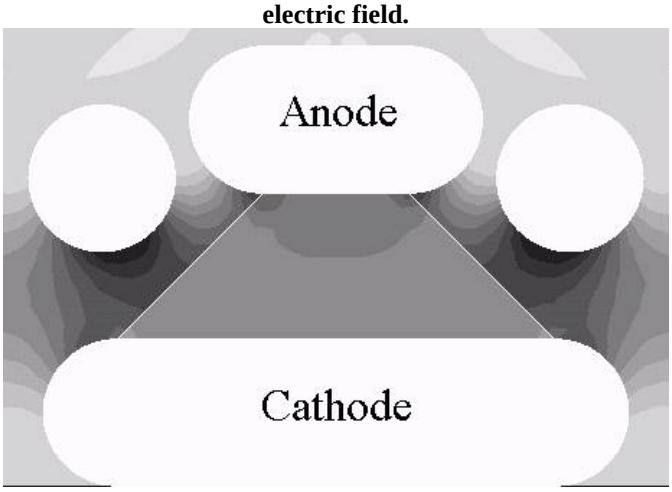

Figure 4: Electric field for a field shaped geometry. The high electric field is much more distributed along the insulator surface.As a result of field shaping, there are

fewer field lines between along the insulator in Figure 4 than in Figure 3 due to the added floating conductor. Figure 5 shows the electric field along the insulator surface with and without field shaping. After field shaping the electric field varies less along the insulator.

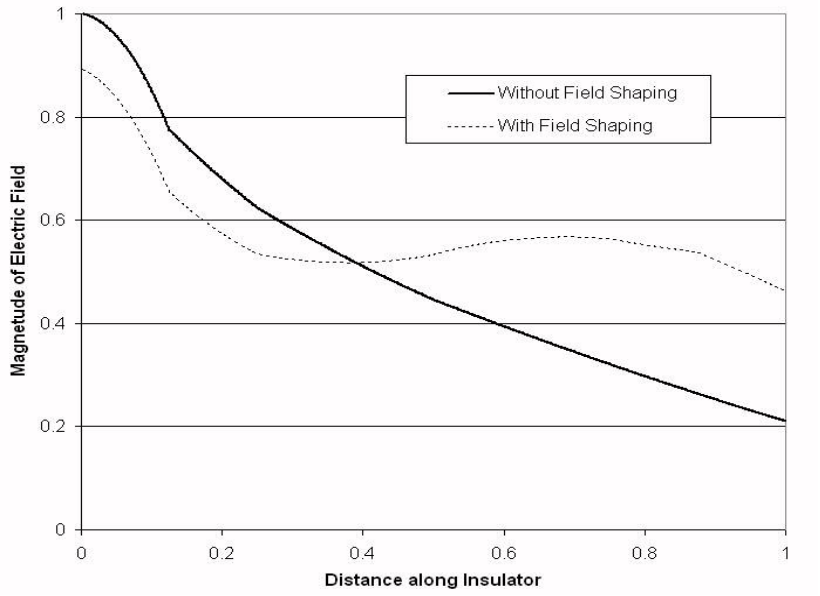

Figure 5: Comparison of electric fields with and without field shaping. The shaped field is more evenly distributed with a lower maximum value.

In high voltage experiments, a triple point is the point at which three regions meet. These regions are usually a conductor, an insulator and a gas, vacuum or fluid [9]. Triple points result in increased electric field as demonstrated in Figure 3. These regions are susceptible as initiating points for flashover because they become sources for electron emission [7]. The rate of emission is proportional to the square of the electric field. Electron emission near an insulating surface, leading to secondary electron emission (SEE), is a cause for the flashover process proposed by Boersch [14]. It has been suggested that controlling SEE can contribute to the largest increase in insulator voltage holdoff [15]. For these reasons, field shaping conductors are often located near triple

points to reduce electric field at the triple point. The electric field near a triple point can be reduced by placing conducting material near the triple point extending into the high voltage region [16]. In many systems this has been shown to increase flashover voltage [9]. This technique is called triple point shielding.

While the general model for flashover is generally agreed upon, experiments have shown the process to commonly initiate in two different ways [17]. This is by electron emission from the cathode or by electron emission from the insulator surface near the anode. These processes are discussed in the next section. In both processes the triple point in that region plays an important role in the initiation. It is important to determine which region in a system has the largest effect on flashover so that appropriate shielding may be implemented.

iv. Flashover by Secondary Electron Emission Avalanche SEEA

Numerous studies have been performed on the vacuum flashover process but many questions remain [18]. The vacuum flashover process generally falls in to one of two categories, cathode initiated or anode initiated. The cathode initiated flashover process was originally proposed by Boersch [14] and has been more thoroughly developed and generally accepted [9]. The anode initiated process is only applied to certain appropriate conditions [9], however, some measurements have shown that anode initiated flashover process can be equally important for +40° to +70° planar insulator geometries [9;17].

Cathode initiated vacuum flashover is generally described by the following steps. The process begins by an emission of electrons from the triple point junction due to field emission or thermal emission [9]. Some of the electrons impact with the surface of the

insulator emitting additional electrons by secondary emission. Again, some of these electrons will impact the insulator surface producing tertiary electrons. This process of Secondary Electron Emission Avalanche (SEEA) quickens as more electrons are emitted and continues along the surface of the insulator until equilibrium is reached.

A secondary electron emitted with energy A_0, will reach a height, y, above the emission point described by eqn. 1 and will travel a distance, x, along the insulator under the applied electric field E described by eqn. 2.

$$y_{\max} = \frac{A_0}{eE_y} \text{ (meters)} \quad [1]$$

$$x_{\max} = \frac{4A_0E_x}{eE_y^2} \text{ (meters)} \quad [2]$$

The total electric field is the combination of the applied electric field and the electric field due to the surface charge. For a zero degree insulator this field is described by eqn. 3 and eqn. 4. The electron path is shown in Figure 6 along with the resulting electric field due to an applied electric field and surface charging.

$$\vec{E} = \vec{E}_x + \vec{E}_y \text{ (V/m)} \quad [3]$$

$$\vec{E}_y = \vec{E}_\sigma \quad \text{(V/m)} \quad [4]$$

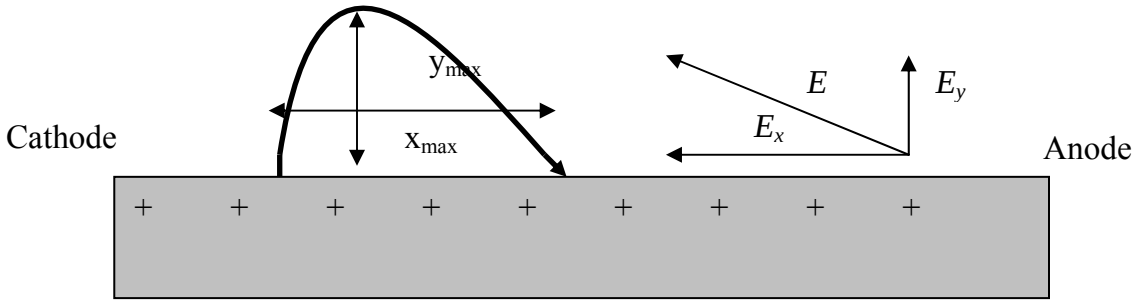

Figure 6: Path of electron and electric field under conditions predicted by Boersch

As secondary electrons are emitted, a net positive charge is left on the insulator surface. The positive surface charge attracts future electrons back to the insulator. Electrons that are emitted from and attracted back to the insulator surface undergo acceleration from the anode-cathode voltage. As the surface charge increases, electrons are more quickly attracted back to the insulator surface. The length of time that secondary electrons are accelerated determines the energy in which they impact with the insulator. An increasing insulator surface charge will result in lower electron energy at time of impact [19]. The impact energy is also dependant on the applied voltage and therefore the distance traveled by the electron as described in eqn. 5.

$$A_i = A_0\left(1+4\left(\frac{E_x}{E_y}\right)^2\right) = eE_y y_{\max} + eEx_{\max} \text{ (eV)} \qquad [5]$$

The electron emission angle affects how far an electron travels along the insulator. Using the law of cosines distribution to describe the emission angle results in electrons that travel half the maximum distance in the y direction, so that eqn. 5 becomes eqn. 6.

$$eE_y y_{\max} + \frac{1}{2} eE_x x_{\max} = A_0 \left(1 + 2 \left(\frac{E_x}{E_y} \right)^2 \right) = A_i \text{ (eV)} \quad [6]$$

This can be used to find a relation between E_y and E_x.

$$E_x = E_y \left[\frac{1}{2} \left(\frac{A_i}{A_0} - 1 \right) \right]^{1/2} \text{ (V/m)} \quad [7]$$

The electric field produced by a surface charge is described by eqn. 8.

$$E_y = \frac{\sigma}{2\varepsilon_0} \text{ (V/m)} \quad [8]$$

Substituting the field from the surface charge into eqn. 7 yields eqn. 9.

$$E_x = \frac{\sigma}{2\varepsilon_0} \left[\frac{1}{2} \left(\frac{A_i}{A_0} - 1 \right) \right]^{1/2} \text{ (V/m)} \quad [9]$$

The number of secondary electrons released is dependant on the energy of the impacting electron. As the energy of the impacting electrons decreases with increased surface charge, the number of emitted electrons per impacting electrons becomes 1. Equilibrium is defined as when the impact energy of the electrons yields only 1 secondary electron so that the insulator charge growth rate is zero [9;19].

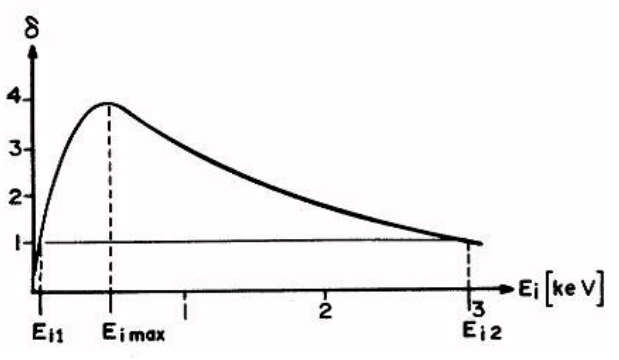

Figure 7: Typical secondary electron emission curve as a function of the energy of impacting electrons [20]

Figure 7 shows a typical curve for the secondary electron yield as a function of the impacting electron energy. The surface charge can then be solved for with the specific impact energy, which yields one secondary electron under the saturation condition according to Figure 7. This surface charge density is shown in eqn. 10.

$$\sigma = 2\varepsilon_0 E_x \left[\frac{1}{2} \left(\frac{A_{i1}}{A_0} - 1 \right) \right]^{-1/2} \text{ (coul/m)} \qquad [10]$$

Once equilibrium has been reached, the maximum current from anode to cathode is limited by the supply of electrons emitted from the cathode and another process must take over in order for flashover to complete [18]. One method used to explain the final stage of flashover includes thermal desorption due to the SEEA electrons creating a conductive plasma on the insulator surface [21]. Another method describes a breakdown process taking place inside the insulating material due to the creation of electron and hole pairs moving into the conduction and valence bands [22]. These methods describe the highly conductive stage that completes the vacuum flashover process.

Anode initiated flashover involves a mechanism similar to bulk breakdown. The process begins by the formation of a small plasma near the insulator surface [17]. This plasma is at a potential equal to the anode either by being connected to the anode or by electron emission. The plasma creates high electric fields tangential to the insulator surface.

The strong electric field results in small breakdown events in the dielectric near the surface of the insulator. The breakdown of the insulator generates new plasma and the process iteratively moves towards the cathode [17]. A tree like pattern forms on the insulator, which branches out toward the cathode, as the small breakdown events form

toward the plasma. When the plasma channel spans the distance from anode to cathode, the final stage of flashover takes place.

v. Magnetic Flashover Inhibition (MFI)

Large pulse power machines frequently require vacuum transmission lines that can withstand intense electrical fields. A proven technique for maintaining a high electric field in a vacuum transmission line is the use of Magnetically Insulated Transmission Lines (MITLs) [8;11]. MITLs are typically two parallel conducting plates insulated by a vacuum. As power flows through the MITL high voltage appears between the plates. At a sufficiently high voltage, electrons are emitted from the cathode and are accelerated across the vacuum gap to the anode contributing to a loss current [11]. When the current through the plates reaches a certain value, the resulting magnetic field begins to affect the paths of the electrons moving across the vacuum gap. When this happens the path of an electron emitted from the cathode is curved in the magnetic field, due to the Lorentz force on the particle, and the electron is pushed back into the cathode [11].

A similar technique may be applied to prevent flashover occurring across insulators. If a properly oriented magnetic field is placed across an insulator surface, any emitted electrons will feel a force away from the surface of the insulator preventing flashover from initiating [11]. Use of a magnetic field in this manner is called magnetic flashover inhibition (MFI). Figure 8 shows an electron path under the influence of MFI. The resulting vector of **E** X **B** must be away from the insulator surface.

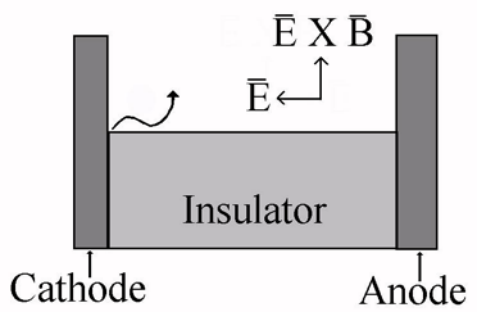

Figure 8: Under MFI, electrons are forced away from the insulator surface.

The important factors that contribute to this effect are the relative strengths of the electric and magnetic fields near the insulator [23;24]. The magnitudes of these fields create the conditions necessary in order for the Lorentz force to have an effect. Eqn. 11 is the force, **F,** on a charged particle with charge, q, and velocity, **v,** in electric field, **E,** and magnetic field, **B**.

$$\mathbf{F} = q(\mathbf{E} + \mathbf{v} \times \mathbf{B}) \quad \text{N} \qquad [11]$$

Experiments have shown that a magnetic field applied from external sources can increase the stress limit of an insulator, delaying flashover [24-26]. For these experiments, a parameter relating the magnitude of the electric field to the magnetic field is generated. If a large current is flowing past the insulator, a self-generated magnetic field may result. In this case, self-generated MFI may occur. This would increase the voltage at which insulators are able to operate without an externally applied magnetic field [27].

The magnetic field for which MFI begins to occur has not been experimentally determined [23]. Calculations have been made to determine the theoretical magnetic field strength at which MFI begins to occur. The critical magnetic field, B_c, is thought to

be

$$B_c = 2.7 \times 10^{-6} \frac{\varepsilon_0^{1/2}}{\varepsilon_1} E_y \text{ T} \quad [12]$$

where E_y is the electric field parallel to the insulator surface, ε_0 is the mean initial energy of the secondary electrons and ε_1 is the impact energy at which SEE yields one electron [24;27]. The ratio of the electric field to the magnetic field (MFI ratio) divided by the speed of light

$$\frac{E}{Bc} \quad [13]$$

is used to determine the initiation point for MFI. For a zero degree insulator, this ratio has been estimated as 0.07 [24].

The standard geometry for most pulsed power insulator barriers is a +45 degree insulator [1]. For +45 degree insulators, the critical ratio for MFI to initiate is thought to be 0.056 [23;24]. However, controlled experiments to determine the effect of MFI on +45 degree insulator geometries have never been conducted [23]. Experimentally finding the relative strength of the electric field and magnetic field at which MFI begins to occur under this geometry will aid in the design of future insulator stack.

Experiment Design

A. Marx Bank Test Stand

Flashover experiments were performed at the University of Missouri Terawatt Test Stand (MUTTS). MUTTS uses 32, 0.7 μF, 100 kV Aerovox capacitors arranged in a Marx bank configuration [28]. The Marx bank was charged by a ± 100 kV, 50 mA Peschel Instruments power supply. It was switched using 16 Physics International T508 spark gaps. The peak erected voltage of the MUTTS facility was 2.8 MV. This bank pulse charged a 7 nF intermediate store capacitor (I-store). An equivalent circuit of the Marx bank and I-store is shown in Figure 9. A vacuum chamber, which contained the test insulator, was connected to the I-store.

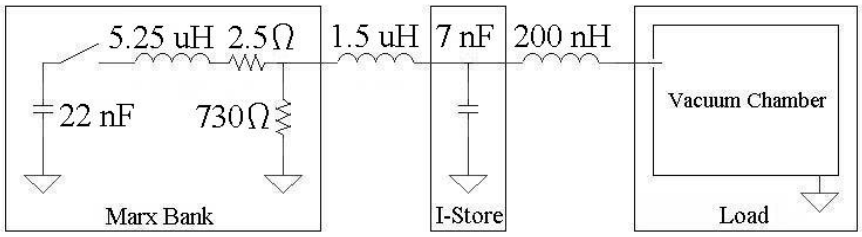

Figure 9: Equivalent Marx bank circuit and placement of vacuum chamber

The Marx bank was triggered by an erected Marx Trigger Generator (MTG) [29]. The MTG was composed of 8, 50 kV, Maxwell capacitors that triggered the first 8 of 16 total Marx bank switches. The mini Marx was bipolar charged by 2 Glassman High Voltage power supplies. The MTG switches were triggered with a Physics International TG-70. The TG-70 provided double its charge voltage, up to 140 kV into a high impedance load at the MTG. The TG-70 was triggered by a Pacific Atlantic Trading Co. PT-55 [30] which was triggered by a 7 kV, PT-003 from an isolated location.

B. Load Design

For flashover experiments, a vacuum load that could be easily installed at MUTTS and adapted for various conditions was needed. A coaxial load was developed to fit this need. When charged, the electric field was easily manipulated while maintaining symmetry. Because the insulator material was translucent, the coaxial geometry also provided a good view of the entire surface where flashover was expected. Figure 10 displays the vacuum chamber with the cathode, anode and insulator inside the vacuum chamber. Figure 11 shows a close view of the insulator region of the vacuum chamber load. The insulator displayed in Figure 11 is insulator geometry "G" in the shot log.

The test chamber was pumped to a base pressure of 5×10^{-6} Torr. This was

accomplished with the use of a Cryo-Torr 100 cryogenic vacuum pump. The base pressure was maintained in the chamber for several hours before testing began.

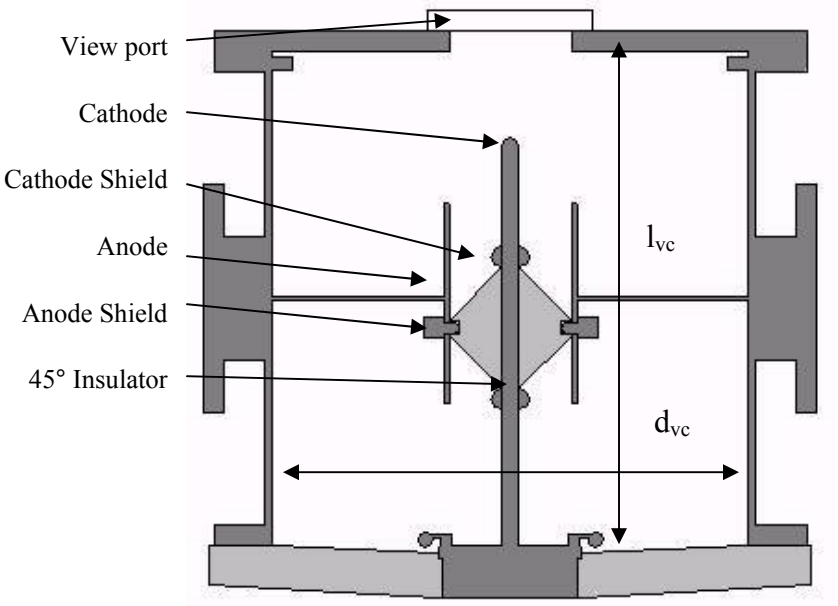

Figure 10: Vacuum chamber interior with shielding added to the triple points for the 45 degree insulator.

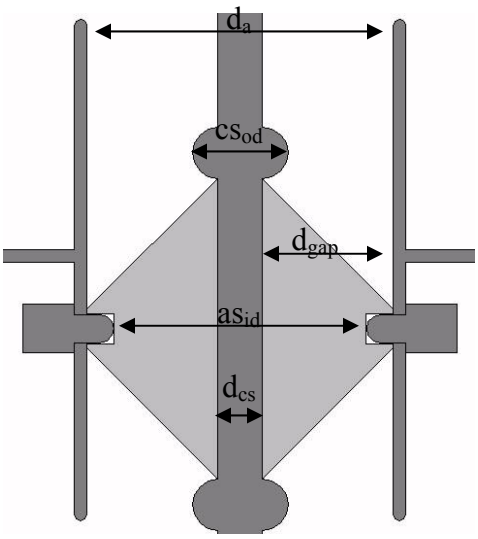

Figure 11: Close view of the test insulator region in the vacuum chamber.

i. Physical Properties

The load included an aluminum vacuum chamber with length, l_{vc} = 61 cm and diameter, d_{vc} = 59 cm. The upper boundary of the load was an aluminum plate with a 15 cm glass viewport. The lower boundary of the load was a plastic barrier with an aluminum conductor running through the center to bring high voltage into the vacuum chamber. A stainless steel cathode stalk, 45 cm in length and with a diameter, $d_{cs,}$ of 2.22 cm, ran through the center of the load.

Two polystyrene test insulators were machined to fit around the cathode stalk. The first had +45 degree interface with the electrodes, the second had a zero degree interface with the electrodes. Figure 11 shows the 45 degree insulator installed with the electrodes and Figure 12 shows the zero degree insulator. The insulator in Figure 12 is insulator geometry "F" in the appendix. Two stainless steel anodes, with lengths 14 cm and 8.5 cm, and an inner diameter, d_a, of 15.24 cm, were machined to fit around the test insulator. The gap distance, d_{gap}, between anode and cathode was 6.5 cm. The anode was connected to the vacuum chamber wall with steel braid.

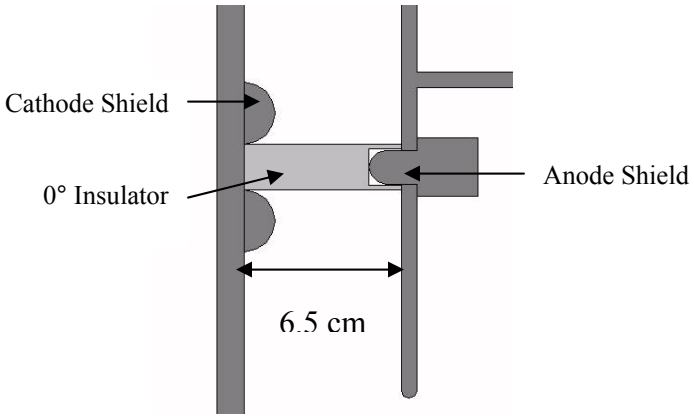

Figure 12: Close view of the zero degree, instead of 45 degree, insulator with shielding added to the triple points. The axis of symmetry is on the left.

Two triple point shields were machined out of aluminum to be place near the anode and cathode triple points. Both anode and cathode shield had a shield radius of 1.3 cm. The anode shield, with length 1.4 cm, was designed to fit between the stainless steel anode pieces. The cathode shield had an outer diameter, cs_{od}, of 4.76 cm which allowed it to extend 1.3 cm into the vacuum gap between cathode and anode. The anode shield had an inner diameter, as_{id}, of 12.57 cm that allowed it to extended 1.33 cm into the insulator material between cathode and anode. A small vacuum gap resulted between the anode triple point shield and the insulator material.

ii. Electrical Properties

The coaxial insulator load described above was placed in parallel with the I-store. The negative pulse from the Marx bank was applied to the cathode at the center of the load. The outside walls of the vacuum chamber were grounded. When the applied voltage was large enough, flashover occurred, effectively creating a short circuit across the insulator.

The insulator gap was designed to have a greater than 99.9% chance of flashover for +45 degree insulators according to experiments done by Elizondo [2]. For a calculation of the acceptable gap length it was assumed that the Marx bank could supply a 2 MV pulse to the insulator gap with a risetime of 578 ns to 89% of the peak voltage. This is possible when no flashover occurs before the I-store reaches peak charge. A 99.9% probability of failure with polystyrene occurs when the average electric field reaches 267 kV/cm. To ensure flashover below 2 MV, the maximum gap length should be less than 7.5 cm. As a result, a 6.5 cm gap length was used to create a high probability of flashover without ever operating above 2 MV.

J.C. Martin's (JCM) equation can be used to predict the peak electric field, F (kV/cm), at which flashover will actually occur for a 45 degree insulator [3].

$$F = \frac{k}{t_{eff}^{1/6} A^{1/10}} \quad [14]$$

For this calculation, the JCM constant, k, was taken to be 210 from [2], t_{eff} is the time to 89% of peak voltage in μs, and A is the insulator surface area, in cm^2. With a 45 degree, coaxial insulator surface, a 6.5 cm gap length, and a 1.11 cm inner radius, the area of the insulator can be found by calculating the surface of a cone according to eqn. 15.

$$\pi\left(r_1 s_1 - r_2 s_2\right) \ (\mathrm{cm}^2) \quad [15]$$

When r_1 is the outer radius, 7.61 cm, r_2 is the inner radius, s_1 is the length of the insulator edge extended to the center of the axis of symmetry and s_2 is the subtracted conical surface length from the cathode to the axis of symmetry, the surface area of the 45 degree insulator is 251.8 cm^2. Therefore the peak electric with a 578 ns applied pulse is expected to be 132.4 kV/cm.

The average pulse length from experimental data was around 250 ns. This would indicate a peak electric field of 152 kV/cm for the experimental data according to eqn. 13. However, the electric field from experimentation was different than this value. The average electric field tended to be near 80 kV/cm and the peak electric field, which occurred at the anode with no triple point shield, was 172 kV/cm. This would indicate that the JC Martin equation does not apply for coaxial geometries.

The capacitance and inductance of the load was calculated for use in circuit simulations. The capacitance of the load was calculated by two methods. The first method was to divide the length of the load into 3 sections and calculate the capacitance

of each section using eqn. 16.

$$C = \frac{2\pi\varepsilon l}{\ln\left(b/a\right)} \quad \text{F} \qquad [16]$$

where C is the capacitance in Farads, l is length, b is outer diameter and a is inner diameter of a coaxial geometry. The total capacitance is the parallel combination of the 3 sections. This method predicted a capacitance of 14 pF below the insulator region, 26 pF at the insulator region, 8.9 pF above the insulator region. The total capacitance would therefore be 48.9 pF. The capacitance calculator of an electrostatic field solver was used to solve for capacitance as a second method [13]. The second method yielded a capacitance of 52 pF. A capacitance of 50 pF was used for circuit simulations of the load.

The inductance of the load section was solved by again dividing the vacuum chamber into three sections, above, below, and at the insulator region. Inductance can be found using eqn. 17 [29].

$$L = \mu_0 l\left\{\frac{1}{8\pi} + \frac{1}{2\pi}\ln\frac{b}{a} + \frac{1}{2\pi\left(c^2 - b^2\right)^2}\left[c^4 \ln\frac{c}{b} - \frac{1}{4}\left(c^2 - b^2\right)\left(3c^2 - b^2\right)\right]\right\} \quad \text{H} \qquad [17]$$

where l is length of the section, a is the diameter of the inner conductor, b is the inner diameter of the outer conductor and c is the outer diameter of the outer conductor. This calculation predicts an inductance of 98 nH below the insulator, 42 nH at the insulator, and 70 nH above the insulator. The total inductance of the load is the series combination of the three sections, 210 nH. However, for flashover events occurring at the insulator, the total inductance does not include the third section above the insulator. In that case the total inductance would be 140 nH.

C. Simulations

Using the values described in the previous section, an equivalent circuit was used to simulate conditions inside the vacuum chamber during operation. The circuit in Figure 9 was used with the vacuum chamber replaced by the values described in the previous section. The vacuum chamber part of the equivalent circuit is represented by Figure 13. As the voltage from the Marx bank charged the I-store, the voltage on the load capacitance increased until flashover occurred. The closing switch was used to simulate when flashover occurs.

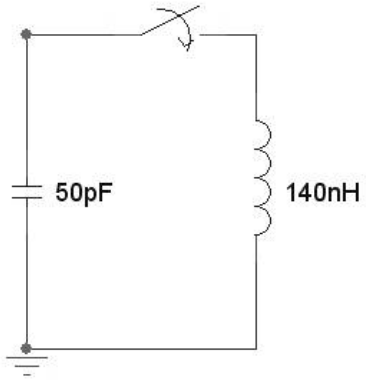

Figure 13: Equivalent circuit of vacuum chamber load

The circuit simulations were expanded to include examining the load as a series of transmission line elements sliced along the length of the vacuum chamber. With this method, the condition at a specific point of the load could be predicted. Using the inductance and capacitance values described, the impedance and electrical length of each section of transmission line can be calculated and inserted into the circuit. The impedance of each section can be described by eqn. 18. The propagation time for each section is described by eqn. 19.

$$Z = \left(\frac{L}{C}\right)^{1/2} \Omega \qquad [18]$$

$$\tau = 2(LC)^{1/2} \text{ seconds} \qquad [19]$$

The circuit model of the load composed of transmission line elements is shown in Figure 14. The length of the load was divided into three sections shown as T1, T2, T3 in Figure 14. T1 includes the region inside the vacuum chamber before the insulator, T2 is the region with the insulator between anode and cathode, and T3 is the region after the insulator at the top of the vacuum chamber. The values of each element were calculated from its inductance and capacitance and are shown in Table 1. The flashover event that occurs along the insulator surface is simulated with a switch between the second and third transmission line elements. In this simulation it is assumed that flashover occurs above the insulator.

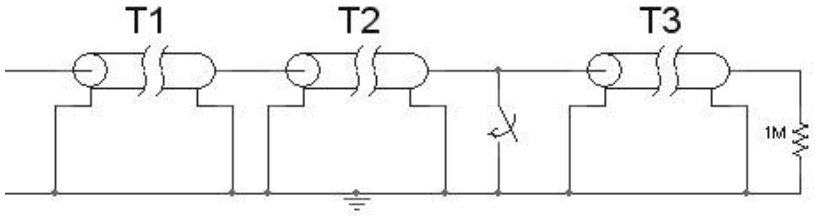

Figure 14: Equivalent circuit of load with transmission line elements

Table 1: Equivalent circuit transmission line values

segment	L (nH)	C (pF)	Z (Ω)	t (ns)
T1	98	14	84	2.3
T2	42	26	40	2.1
T3	70	9	88	1.6

PSpice simulations of the complete circuit were used to predict how the voltage would appear at the insulator surface. As the Marx bank switched its energy into the I-

store, the voltage across the insulator rose to about the same level as the I-store. The surface of the insulator would flash at a certain voltage and create a short circuit. At this point the voltage would ring between the various elements of the load and the I-store. This ringing could be high enough to initiate flashover elsewhere in the vacuum chamber late in time and this was found to be the case through experimentation.

Figure 15 shows the result of a PSpice simulation of the flashover event occurring in the load. The simulation was performed by using transmission line elements. Three different points in the circuit are displayed. The insulator voltage is the point where flashover is designed to occur first. The vacuum barrier is the plastic barrier that separates the vacuum chamber from the oil above the I-store. The probe is at the point where voltage measurements were made with the diagnostic described in the next section. Although all three points have a similar charge time and peak voltage prior to flashover, there is a significant difference in the shape of the voltage afterwards. This simulation takes into account a second flashover event that was viewed at the vacuum barrier after the primary flashover event occurs. While the exact shape of the voltage at the scope depends on the time and resistance of the second flashover, the simulated probe voltage shape is similar in shape to data from the experiment. A plot of the voltage from a typical shot is included in Figure 15.

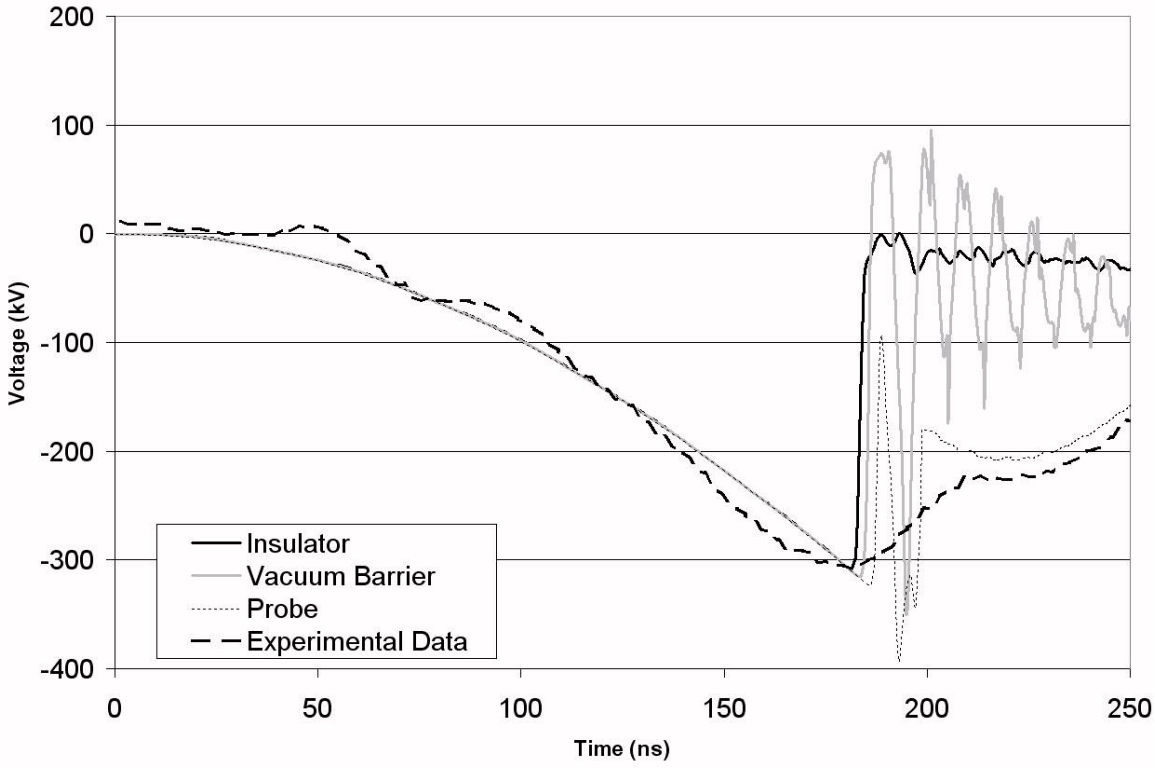

Figure 15: Spice simulation of voltages at three different points at load

The electric field inside of the vacuum chamber was found by inserting voltages from a circuit simulation into an electrostatic field solver and solving for the specific geometry. This process was performed for both 45 degree and zero degree insulators for each triple point shield scenarios. The effect that the triple point shield had on the electric field along the insulator surface was examined.

When triple point shields were applied to the cathode and anode, the electric field on the insulator surface in that region decreased. As a result the electric field increased in the middle region of the insulator. Figure 16 shows the magnitude of the electric field on the surface of the insulator for the zero degree insulator and the 45 degree insulator with no triple point shields applied. Figure 17 shows the zero and 45 degree insulators with the triple point shields applied to both cathode and anode. These electrostatic simulations

were performed by applying -300 volts to the cathode.

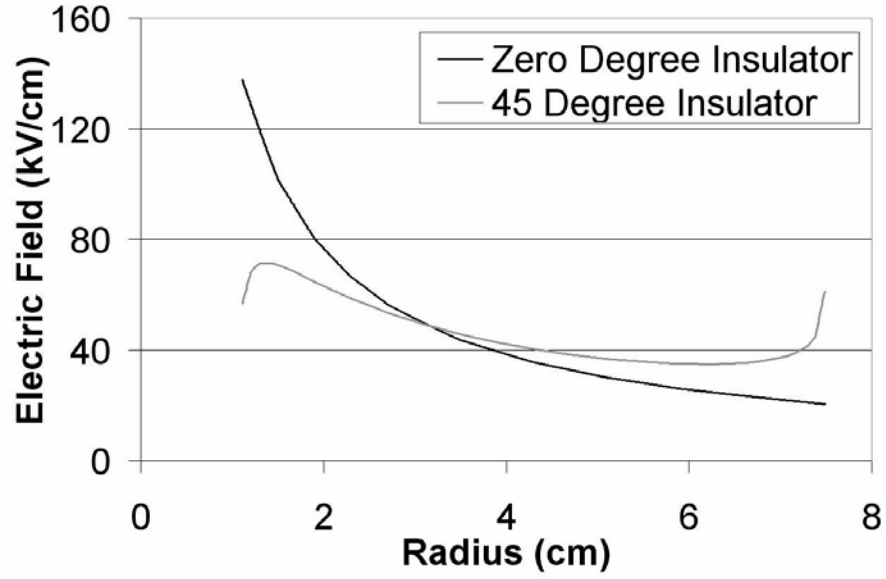

Figure 16: Electric fields with 300 kV applied voltage for zero and 45 degree insulators with no triple point shield

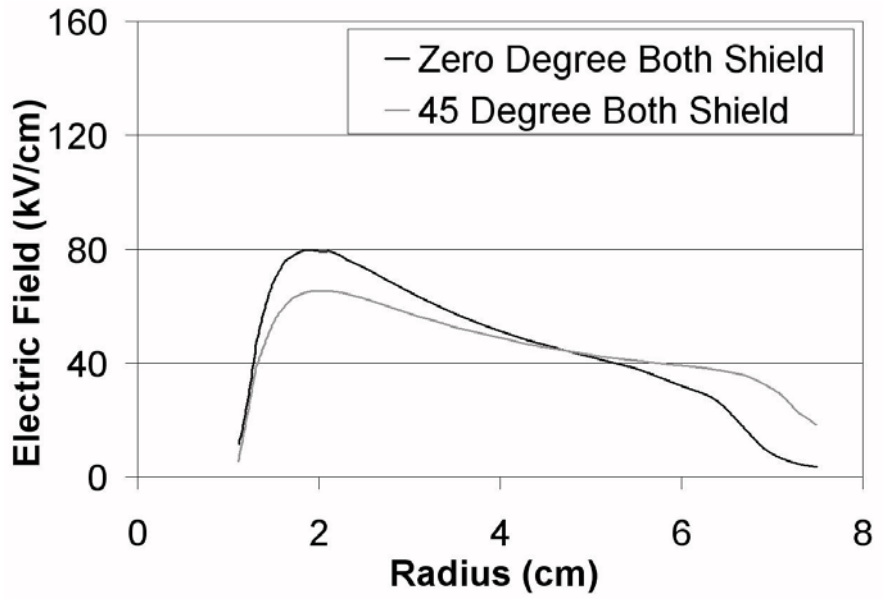

Figure 17: Electric fields with 300 kV applied voltage for zero and 45 degree insulators with triple point shields at anode and cathode

D. Diagnostics

Voltage measurements were made on the cathode using a water resistor voltage

divider with a division ratio of 21600 to 1. A glass view port at the top of the vacuum chamber was used to view the surface of the tested insulator. A digital camera placed above the vacuum chamber took open shutter pictures of the flashover process. Pictures were used to verify that flashover had occurred and that data acquired was to be considered "good." To determine the beginning of the flashover event, a Hadland Imacon 200 digital framing camera was utilized. The framing camera provided time resolved pictures of flashover on the insulator. Other diagnostics were used to measure voltages and currents on the Marx bank system. These diagnostics are described in [30].

E. MFI Design Considerations

The coaxial load was designed with the consideration of future high current flashover tests. These tests would be used to study the initiation of self-generated MFI on high voltage insulators. For these experiments, current must be flowing past the insulator surface prior to flashover. The placement of a resistance between the anode and cathode would allow current to flow past the insulator while voltage is applied across the insulator. By varying the resistance, the voltage and current can be modified with respect to each other. With the current and voltage, it is possible to calculate the electric and magnetic field inside the vacuum chamber between anode and cathode.

The electric field at the insulator can be described by

$$E = \frac{V}{\ln\left(\frac{b}{a}\right) r} \text{ V/m} \qquad [20]$$

where V is voltage, a is inner conductor radius, b is outer conductor radius, and r is the variable position along the radius between the conductors.

The magnetic field at the insulator can be described by

$$B = \frac{\mu_0 I}{2\pi r} \quad \text{T} \qquad [21]$$

Where I is current, and r is the variable position along the radius between the conductors.

The ratio of the electric to magnetic field can be solved as

$$\frac{E}{Bc} = \frac{V 2\pi}{\mu_0 I \ln\left(\frac{b}{a}\right) c} \qquad [22]$$

where c is the speed of light. Because both electric and magnetic field depend inversely on the radius for a coaxial load, the ratio of the quantities does not depend on radius. As a result, the coaxial minimizes the variation of the electric to magnetic field ratio (MFI ratio) between the conductors. This allows for an examination of a specific MFI ratio for each flashover event.

As discussed in section 1, the initiation of MFI may begin at the predicted MFI ratios for zero degree and 45 degree geometries. To examine this hypothesis for a zero degree insulator, flashover should be tested above and below the MFI ratio of 0.07, and for a 45 degree insulator, flashover should be tested above and below the MFI ratio 0.056. For both situations, MFI should begin to hold off flashover as the ratio goes below the predicted value.

Circuit simulations showed that by changing the load resistance of the experiment from 4 ohms to 10 ohms, it is possible to test over the predicted ratios. Figure 18 and Figure 19 demonstrate the effect that changing the load resistance has on the MFI ratio for the coaxial load. For both zero degree and 45 degree geometries, the MFI ratio goes below the predicted value as the resistance is decreased. For Figure 18 and Figure 19 the

predicted MFI initiation ratio is represented by a dashed line.

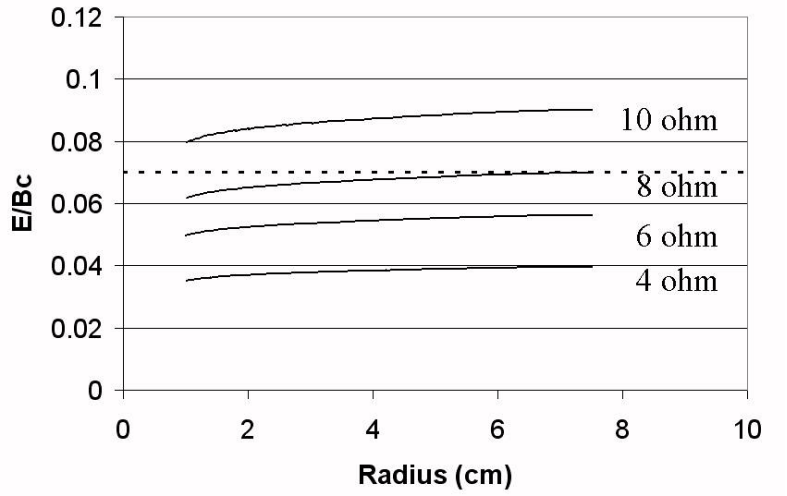

Figure 18: MFI test ratios for a zero degree insulator

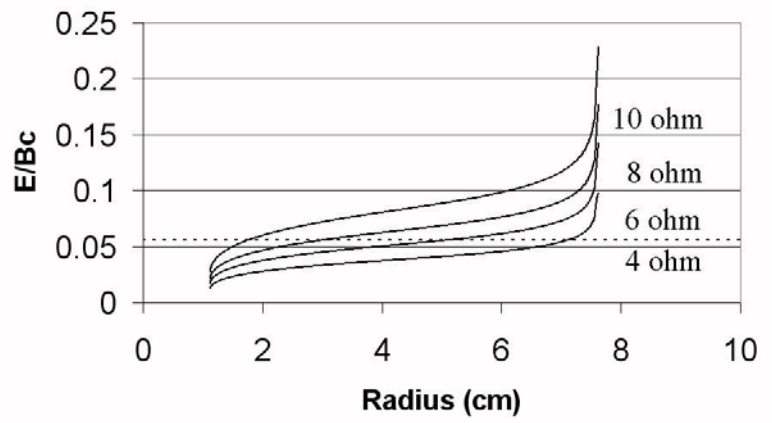

Figure 19: MFI test ratios for a 45 degree insulator

To perform the high current MFI tests on the current test stand, it would be necessary to add a switch between the I-store and vacuum chamber. This would sharpen the pulse and increase the current past the insulator to the levels required for MFI.

Flashover Testing

A. Statistical Shot Plan

Data were taken on both zero and 45 degree insulators with various triple point shields. The insulators were tested with no triple point shielding, with both triple points shielded and with each triple point shielded alone. In total, 452 open circuit shots were taken on the various insulator geometries. Many of these shots were used to try to discern a test setup and geometry that could be used in a complete statistical experiment. A complete shot log is listed in the appendix. Once a specific 45 degree and zero degree insulator geometry were determined for the experiment, Figure 11 and Figure 12 respectively, a statistical shot plan was developed.

For the shot plan, the various triple point shield treatments for the 45 degree insulator and the no shield treatment for the zero degree insulator were tested in a randomized complete block experiment. The purpose of the randomized complete block design is to ensure that each treatment be used in every possible configuration. This forces the cathode triple point shield to be used with and without the anode triple point shield and vice versa.

Another advantage of the randomized complete block design is that it can remove a variable from the main effects of a model. The design was used to mitigate the effect of uncontrolled experimental parameters like risetime or chamber pressure which may vary slightly with time. For insulator flashover tests, the number of shots taken on an insulator can also have an effect on flashover voltage. In order to remove these variables from the model, multiple blocks can be performed in the experiment. Each complete block contains every combination of the treatments in a randomized order. The goal of this experiment design is to test for the effect that triple point shielding has on an insulator without including the effect that time or number of shots has on flashover voltage.

Data from multiple test blocks were collected with the triple point shield location factor randomized within the block and time as the blocking variable. Any effects of these variations on the factor of interest (flashover voltage) were not correlated with the data. For a balanced design, when r = number of times each setup is tested, t = number of treatments, and k = number of treatments per block, λ must be a whole number [31].

$$\lambda = r\frac{(k-1)}{(t-1)} \qquad [23]$$

For this experiment it is desirable to minimize the number of times that the

vacuum chamber has to be opened to change the triple point shield, and then pumped to a low pressure. This is due to the large amount of time it takes to perform those steps. With 5 treatments per block, and 5 total treatments the number of times each setup is tested should be greater than 1 to block for time. By taking 2 randomized complete blocks, the total number of times that the vacuum chamber should be opened and pumped down is N = r*t = 10.

The treatment order of the experiment was randomly determined within each block in order to ensure that the shot number was not correlated with the data. The treatment order is shown in Table 2. Shot numbers 307 through 452 were used to create the randomized complete block test.

Table 2: Randomized complete block design treatment order

Treatment	block 1 order	block 2 order
45 degree no shield	3	1
45 degree cathode shield	1	4
45 degree anode shield	2	5
45 degree both shield	4	2
zero degree no shield	5	3

Each treatment was tested twice with about 15 shots per experiment. Analysis of the standard deviation of early shots indicated that with a total of around 20 shots per treatment the data would be normal. The total number of acceptable shots per treatment was about 25 after the both blocks were performed due to some shots having problems that render the data unusable.

B. Data accumulation

A complete shot log is listed in Appendix A. Figure 20 shows a typical shot, which had a risetime of about 250 ns and a flashover voltage of near 300 kV. Two

voltage peaks of similar magnitude were frequently measured on the same shot. To determine the beginning of the flashover event, a framing camera was utilized. The framing camera provided time resolved pictures of flashover on the insulator. Each frame is a 500 ns exposure as shown on the time scale in Figure 20. The four pictures in Figure 21 correspond to the four periods of time indicated in the voltage signal.

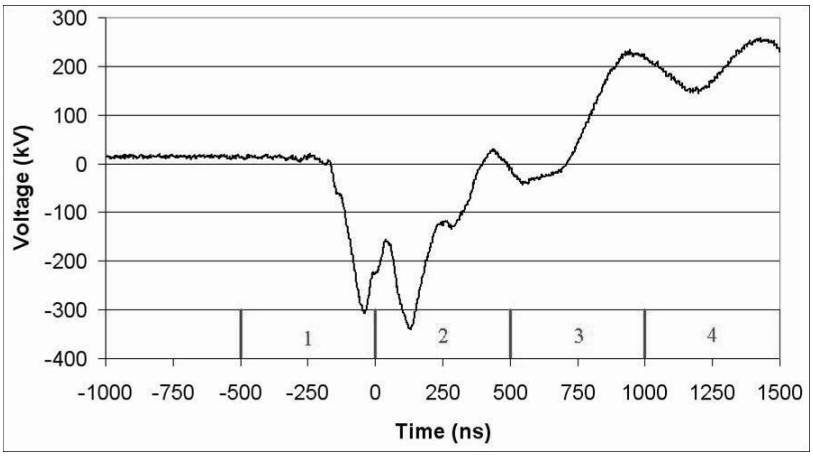

Figure 20: Typical I-store voltage for a single shot. Photograph exposure times are labeled.

The framing camera images show that flashover begins during the first frame. This is indicated by the bright points at the anode and cathode of the insulator. This corresponds to the first voltage peak in Figure 20. Flashover on the test insulator always occurred on this initial rise in voltage. After the initial flashover voltage signals ring between the load and I-store and the signals are seen on the probe. Late-time discharges occur on the load and throughout the vacuum chamber as a result.

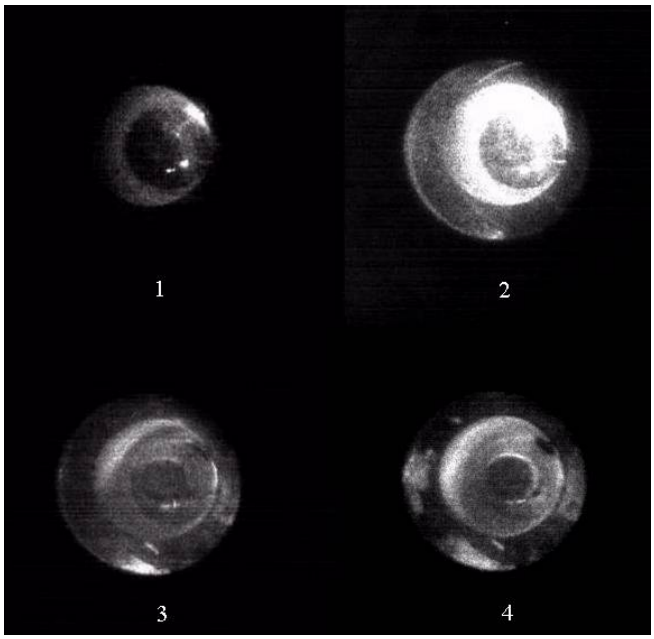

Figure 21: Framing camera showing consecutive images of the same shot, 500 ns per exposure. Exposures correspond to timing displayed at bottom of Figure 20

A glass view port at the top of the vacuum chamber was used to view the surface of the tested insulator. Open shutter, time integrated pictures of the flashover event were taken with a digital camera. Pictures were used to verify that flashover had occurred. Figure 22 shows a typical shot of the insulator with plasma forming across the surface and bright spots near the cathode and anode triple points.

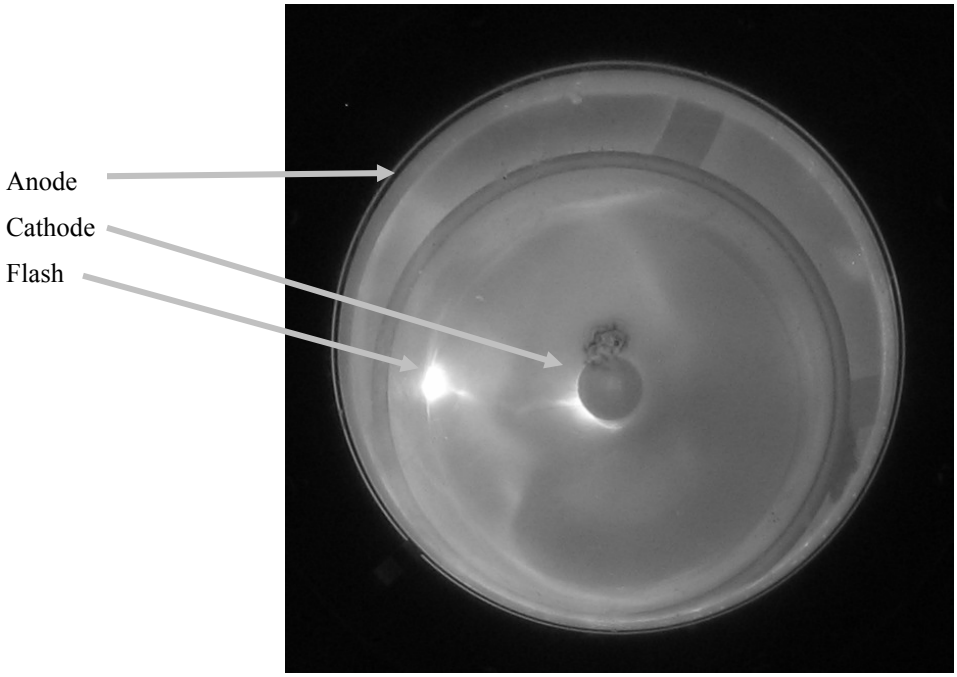

Figure 22: Flashover on insulator surface taken with digital camera

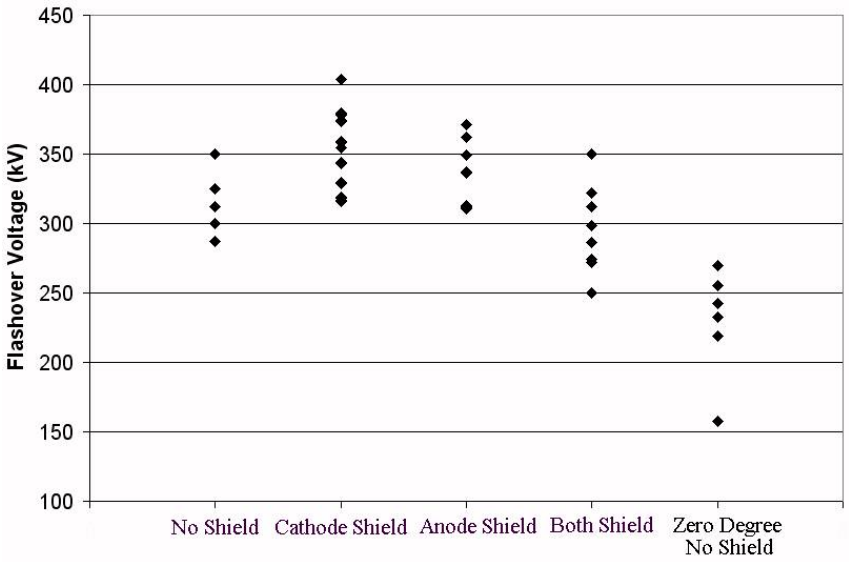

Figure 23: Flashover voltages on the 45 degree insulator for no shield, cathode shielded, anode shielded, both anode and cathode shielded, and zero degree no shield.

After the shots were performed the peak voltage, risetime and other values for each shot was tabulated with Matlab. The complete script that was created for this purposed is in Appendix B. Figure 23 displays the flashover voltage of the 45 degree

insulator under the different shielding arrangements. It includes the data from the zero degree insulator.

The flashover voltage of the 45 degree insulator was generally higher than the zero degree insulator. The 45 degree cathode shield and the anode shield, applied individually, both showed an increase in flashover voltage over the no shield case. However, when both cathode and anode shielding were applied together, the flashover voltage dropped below the no-shield condition.

Analysis

A. Flashover voltage comparison

After the tests were completed the mean flashover voltage of each treatment was calculated and compared. Averaged over all shielding cases, the 45-degree insulator had a mean flashover voltage of 320 kV. The zero-degree insulator had a mean flashover voltage of 230 kV. The mean flashover voltage of each shielding configuration was also recorded. A summary of the each shield treatment and the resulting mean flashover voltage along with electric field at the anode and cathode triple point is provided in Table 3. The electric fields were obtained from electrostatic simulations using experimentally acquired voltages.

Table 3: Resulting electric fields and voltages on the sample of polystyrene with each triple point shielding treatment

Treatment	Cathode triple point E-field magnitude (kV/cm)	Anode triple point E-field magnitude (kV/cm)	Average E-field (kV/cm)	**Flashover Voltage (kV)**	**Standard Deviation (kV)**
45° No Shield	56	172	81	**308**	**18**
45° Cathode Shielded	< 1	208	92	**350**	**26**
45° Anode Shielded	68	86	86	**337**	**23**
45° Both Shielded	< 1	110	71	**285**	**23**
0° No Shielded	35	45	35	**230**	**24**

These data were analyzed with Statistical Analysis Software (SAS) [32] using a generalized linear model procedure. If successful, a generalized linear model would allow the flashover voltage to be described by the variables in the experiment as part of a linear model. Two models were examined with SAS and they are described by Eqns. 23 and 24. The generalized linear model procedure uses an analysis of variance (ANOVA) to determine how well the model can describe the flashover voltage. A flowchart of the analysis that was performed is shown in Figure 24.

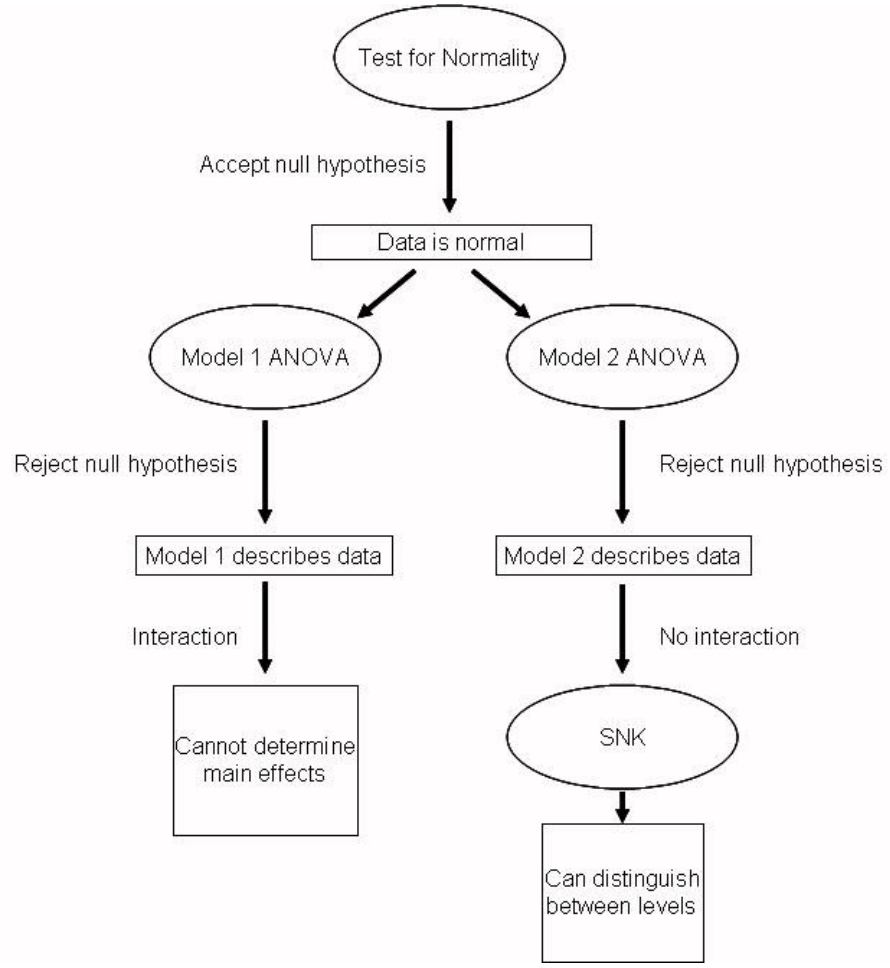

Figure 24: Flowchart of statistical analysis

For the analysis, several hypothesis tests were performed. These tests were performed with $\alpha = 0.05$, to create a confidence interval, $1-\alpha$, of 0.95 or 95%. If the population mean can be described by μ, the sample mean will be in the confidence interval, with $1-\alpha$ confidence. The confidence interval describes the level of confidence that the mean of a random sample of data will be found within a certain range.

A generalized linear model procedure creates a function that can predict the change of the dependant variable, flashover voltage, due to the treatment. This procedure uses ANOVA to determine the variance of the dependant variable due to random error

and due to the treatment. The ANOVA procedure tests the variance of the dependant variable by testing the null hypothesis that the means of several normal distributions are all the same. The null hypothesis is rejected with 1-α confidence if the means are not the same [35].

One goal of the generalized linear model is to determine the main effect of an independent variable. The main effect is the effect that an independent variable, shield type, has on the dependant variable, flashover voltage. If an interaction occurs between independent variables in a model, the main effect that one independent variable has on the dependent variable cannot be determined.

ANOVA assumes that the data are normal. A Shapiro-Wilk hypothesis test was used to test the data for normality because it is an appropriate test for samples sizes near 50 [30]. The test provided a p-value of 0.3525 while testing at the 95% confidence level. Because this value is larger than .05, the null hypothesis for normality cannot be rejected, and the data is normal. Therefore a generalized linear model can be used to test the effect that the treatments have on flashover at this confidence level.

The first generalized linear model (model 1 in Figure 24) applied the cathode and anode shield as separate variables; each variable has two states: with or without the shield. When C is cathode shield and A is anode shield, then the flashover voltage, FV, is shown in Eqn. 24. The term C*A describes a possible interaction between the two main effects. The analysis of variance, performed by SAS, concluded that the null hypothesis, all flashover means are equal, could be rejected [33;34].

$$FV = C + A + (C * A) \qquad [24]$$

The flashover voltage in the model depended on either treatment as a main effect

and the model described the flashover voltage at a 95% confidence level. However, the model also provided a p-value for the interaction term of less than 0.0001. The interaction of the cathode shielded and anode shielded treatments was statistically significant at the 95% confidence level. The significant interaction meant that for both treatments, cathode shield and anode shield, the effect that one treatment had by itself could not be distinguished from the other treatment. How one treatment affected the flashover voltage depended on the state of the other treatment. Because of the interaction between the treatments in the first model, the main effects, either anode shield or cathode shield could not be determined.

While keeping in mind that the interaction term was significant, a second model (model 2 in Figure 24) was analyzed that described the shield treatment as a single variable with 4 states: no shield, cathode shield, anode shield and both shield. The flashover voltage in this model depended on the state of both triple point shields at the same time and is described by

$$FV = shield\_type \quad [25]$$

With this type of model, the entire state of each treatment is part of the main effect that describes flashover voltage. Changing one part of the treatment, i.e. Cathode shield, by itself needs to be considered with the state of the anode treatment. There is no interaction term because there is only one main effect. The analysis of variance showed that this model also described the flashover voltage at a 95% confidence level with a p-value less than 0.0001.

Because this model describes flashover voltage with only the main effects, it allowed an extension of the analysis with a Student-Newman-Keuls (SNK) test to clearly

show which treatments differed from the others [31]. The SNK test is a way to rank the means of a group based upon how far apart the means are. This provided a ranking of the flashover voltages according to the shield treatment.

Using a SNK test on the means, with α=0.05, the only cathode and only anode shielding treatments were both shown to be statistically higher than the unshielded and simultaneously shielded treatments. However, the only cathode and only anode shielding treatments were indistinguishable from each other with the SNK test. Similarly the unshielded and combined shielding treatments were indistinguishable with the SNK test. Two groupings were formed by the SNK test, the higher flashover voltage group, with both single shield treatments and the lower flashover voltage group, with the no shield treatment and the both shield treatment.

B. Electrical field comparison

A comparison of the electric fields along the surface of the insulator began with electrostatic simulations of the fields inside the vacuum chamber. The purpose of these comparisons is to try to determine what caused a difference in flashover voltage between shielding conditions. The mean voltages of each shield treatment were used to create a plot of the resulting field with the use of Maxwell SV [13], an electrostatic field solver. Figure 25 shows the equipotential plot inside the vacuum chamber with a 300 kV applied voltage between cathode and anode. In Figure 25, the anode and cathode triple point shield reduce the change of voltage per distance near the insulator, reducing the electric field in their respective regions.

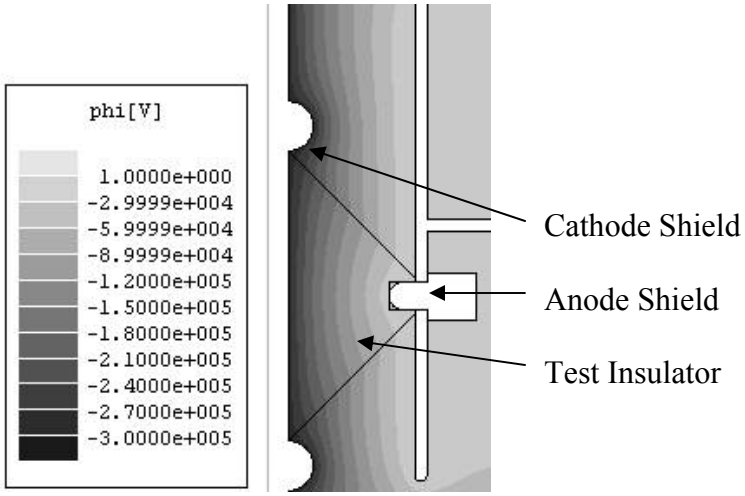

Figure 25: Simulated equipotential plot of load with cathode and anode shields. The voltage applied to the cathode is -300 kV. The axis of symmetry is on the left.

Figure 26 shows the simulated magnitude of the electric field along the surface of the insulator under the different shielding arrangements. The distance on the insulator increases while moving away from the cathode triple point so that 0 cm corresponds to the cathode triple point and 6.5 cm corresponds to the anode triple point. These values were obtained by inserting the acquired flashover voltage into an electrostatic field solver transforming the voltage magnitude into electric field vectors. This transformation allows for an easy comparison with past studies on shielding. This method shows the effect on the electric field due to the insulator and shield geometry but does not include the effect of surface charging on the insulator. The simulations indicated that adding a cathode shield decreased the electric field at the triple point significantly. Adding an anode shield also decreased the electric field near the anode. Outside of the shielded regions, the electric fields remained very similar.

Table 3 shows the electric field that occurs at the triple point of each treatment type as a result of the electrostatic simulations. A field of less than 1 kV/cm is indicated

in instances where the simulation indicated a very small but nonzero electric field. Also shown is the average electric field across the insulator for each treatment. The ranking of the average electric field for each treatment follows the flashover voltage. Cathode shield and anode shield both have the highest average electric field while the no shield and both shield treatments have the lowest average electric field.

The electric fields at which flashover occurred for the zero degree insulator were lower than the electric field for the 45º insulator. This was expected as discussed in section 1. The average electric field was at least twice as large for all of the 45° insulators.

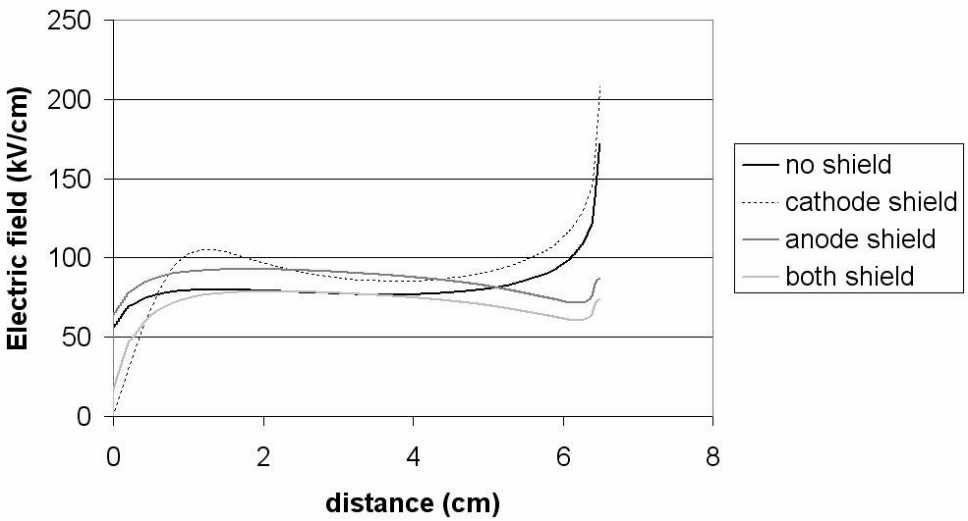

Figure 26: Electrostatic simulations using the acquired flashover values provide plots of the electric field along the surface of the 45 degree insulator for multiple shielding arrangements. The cathode triple point is located at position 0 cm and the anode triple point is located at position 6.5 cm.

The magnitude of the electric field for the cathode shield and anode shield are slightly higher but similar near the center of the insulator than for both the no shield and both shield geometries. The addition of triple point shields will result in a higher electric field at a different location on the insulator surface. This shift may have caused the

electric field at the center of the insulator to approach a critical value in which flashover will occur regardless of the field at the actual triple point.

Figure 27 and Figure 28 shows the tangential and normal electric field on the surface of the insulator. Both the tangential and normal field exhibit similar qualities to the electric field magnitude. The cathode shield decreases the field near the cathode triple point and the anode shield decreases the field near the anode triple point. However, for the tangential electric field, near the cathode, the effects from the cathode shield do not extend far along the insulator material. The lowered electric field reaches less than 0.5 cm along the insulator. For the normal electric field, the reduction from the cathode shield extends over 1 cm. Near the center of the insulator, the highest tangential electric field is on the anode shielded insulator and the highest normal field is on the cathode shielded insulator. At the anode, the effects of the shield again reach further into the material for the tangential electric field than for the normal electric field.

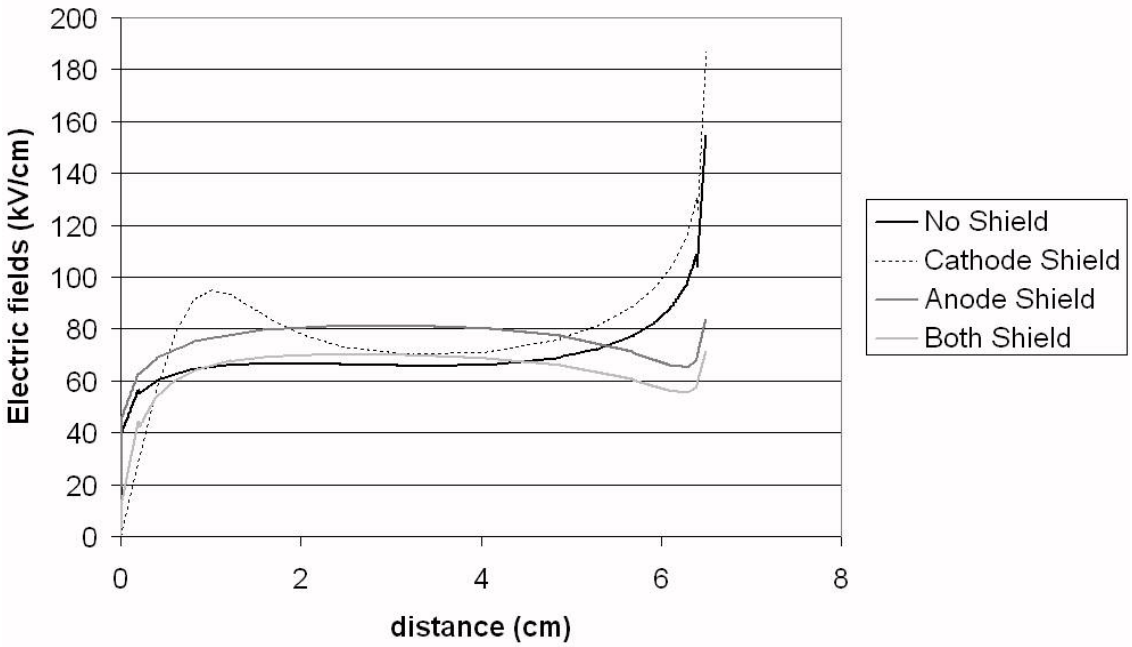

Figure 27: Electric field tangential to the 45 degree insulator surface. The cathode triple point is located at position 0 cm and the anode triple point is located at position 6.5 cm.

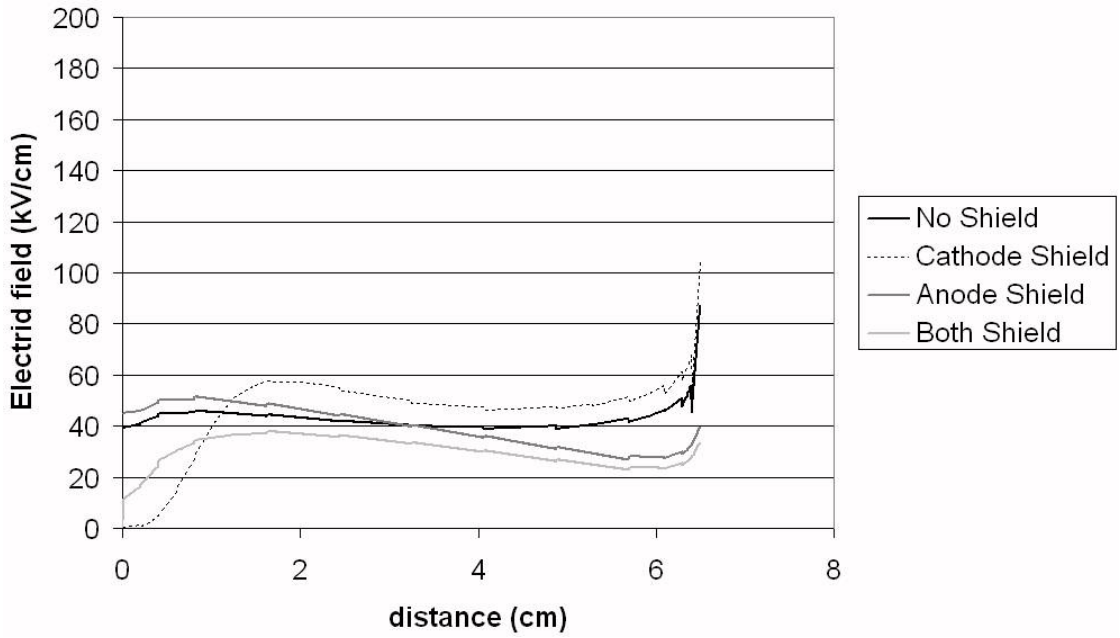

Figure 28: Electric field normal to the 45 degree insulator surface. The cathode triple point is located at position 0 cm and the anode triple point is located at position 6.5 cm.

In other recent flashover experiments, tests have shown that flashover is most likely to initiate at the anode triple point for 45 degree insulators [1]. This is due to electron emission from the insulator surface near the anode increasing the electric field and resulting in breakdown events moving from the anode toward the cathode. The increased flashover voltage resulting from shielding the anode triple point would support this claim by decreasing the electron emission from the insulator surface. In addition, the coaxial geometry produces a larger electric field near the cathode than a planar geometry. The significant increase in flashover voltage for the cathode shield treatment may be attributed to minimizing the enhanced cathode electric field for a coaxial geometry. As a result both anode and cathode triple points can highly contribute to the flashover of a 45 degree coaxial insulator.

The reduction in flashover voltage after adding both an anode and cathode shield is different than the results in [1]. Because [1] was performed with a planar geometry, it is possible that the role of interaction between coaxial geometry triple points is different than for planar geometries.

As a result of keeping the anode triple junction directly against the insulator surface, a small void was formed between the anode shield and insulator for anode shielded tests. The authors of [1] describe using small gaps between the insulator and conductor at the triple point junctions to ensure that the shield material was fitted against the insulator. It is possible that the void formed near the anode shield might affect the flashover when the cathode triple point shield is shielded. This would indicate that the lower electric field from the cathode triple point shield is decreasing the role of the cathode triple point and causing the conditions at the anode to have a larger effect on flashover.

Conclusion

A. Summary and Conclusions

Increasing performance of vacuum insulator barriers is a common goal in pulsed power. Insulating performance is continually being improved while new methods are developed. Many experiments have been performed in order to fully understand the process of flashover. Triple point shielding techniques have been shown to increase flashover voltage, but the role of cathode vs. anode shielding is still not fully understood.

This thesis described an experiment that was performed on flashover in a coaxial geometry. The design and construction of the test stand was presented and an analysis of data gathered for the coaxial geometry was demonstrated. The experiment provided insight on the role of triple point shielding for coaxial geometries and the following conclusions were made:

- For coaxial geometries, +45º insulators have a higher flashover voltage than 0º insulators.

Table 3 shows that the 0º insulator flashover voltage was much lower than the 45º insulator flashover voltage. This result has been demonstrated many times for planar insulator geometries and was expected for the coaxial geometry. One reason for this is because the region near the cathode triple point for a +45 degree insulator has a reduced electric field as shown in Figure 16.

- Adding a cathode triple point shield or an anode triple point shield will increase the flashover voltage for some coaxial geometries.

Shielding either triple point, anode or cathode, has been shown to increase the flashover voltage of the insulator over the no shield case. This result is also shown in Table 3. The electric field at both the anode and cathode triple point has an effect on insulator flashover.

- The 45-degree coaxial flashover experiment showed that triple point shielding needs to be carefully considered before being implemented.

Applying a shield to both triple points can decrease the flashover voltage compared to a single shield and can result in no voltage increase over the unshielded case. The interaction of the shielding has an effect on flashover so that the states of both triple points need to be considered simultaneously. Both triple point regions were found to be important and dependant on each other for some coaxial geometries.

- The role of triple point shielding for some coaxial geometries is different than planar geometries.

For coaxial geometries, the interaction between cathode and anode triple point shielding is important. Specific negative effects of one type of shielding may not be present until both triple points are used. This has not been shown to be the case for planar geometries. The interaction may be more apparent for small radius coaxial geometries similar to the setup used in this experiment. Because the electric field has large 1/r dependence, a coaxial geometry with a larger inner and outer radius may behave more like a planar geometry.

- The surface charge that forms for a 45 degree coaxial insulator may affect the role of triple point shielding differently than for a planar geometry.

The charge that forms on the insulator surface is affected by the initially applied electric field. This electric field is a function of both the insulator geometry and application of triple point shields. As shown in Figure 16 and Figure 17, the electric field for a 45 degree coaxial insulator is intricate due to the 1/r effect that increases the field at the cathode and the +45 degree effect that increases the field at the anode. The surface charge profile may become highly unbalanced due to these effects and could contribute to high electric fields that are not represented in the electrostatic simulations. This may explain why the combined triple point shield produced unexpected results. The surface charge profile could be examined to view how it changes the electric field for the 45 degree coaxial insulator.

- For a coaxial geometry, it is possible to experimentally determine the critical magnetic field needed to initiate MFI.

Because both the electric field and magnetic field have 1/r dependence, the ratio of the electric field to the magnetic field does not change over the length of this insulator. This is shown in Figure 18 and Figure 19. The critical magnetic field ratio was within the range that was testable in the experiment design.

Accomplishments in this study included the design and construction of a high voltage vacuum flashover test stand. The test stand was useful due to its ability to be easily changed in order to test flashover in many configurations. Testing has given insight to coaxial flashover events and provided information useful for future high current experimentation.

B. Future work

In the design of this test stand, future high current experimentation was heavily considered. The vacuum chamber was connected to a Marx bank so that the energy necessary for high current experiments was available. The insulator was designed to withstand the higher voltages that would result from shorter pulse lengths in a high current test. These attributes were included for the purpose of finding a critical electric to magnetic field for which MFI begins to occur. Finding the electric field to magnetic field necessary to initiate MFI for a 45 degree insulator would be a significant contribution to the design of future pulsed power machines.

The analysis of the electric field on the insulator surface was performed without considering the additional field formed by surface charging. Because a measurement of the surface charge would be extremely difficult, the measurement was not feasible for

this experiment. The analysis could be expanded by measuring or simulating the charge formed on a coaxial insulator surface. While the applied electric field is the factor that is investigated in many flashover studies, the resulting electric field from surface charge equilibrium may provide insight on how the initiation of flashover takes place for a coaxial geometry.

Appendix A: Shot Log

Shot #	Insulator geometry	Shield type	Marx Charge (kV)	Marx Pressure (psig)	Chamber Pressure (Torr)	notes	Risetime 10-90%	Risetime (ns)	Max Voltage	Peak (kV)
1	**A**	**N**	26	Air 5	3.00E-05	no pic	4.24E-07	424	8.64E+04	86
2	**A**	**N**	26	5	3.00E-05	no pic, bad data				
3	**A**	**N**	26	5	2.00E-05	added 2x current attenuation, no data				
4	**A**	**N**	26	5	2.00E-05	no current attenuation	2.66E-07	266	1.90E+05	190
5	**A**	**N**	26	5	1.50E-05	pic of tank	2.74E-07	274	1.90E+05	190
6	**A**	**N**	26	5	5.00E-02	pic of tank, no data				
7	**A**	**N**	26	5	5.00E-02	pic of tank, **marx voltage**, DPL	1.68E-07	168	4.06E+05	406
8	**A**	**N**	26	5	5.00E-02	first pic, no flashover, no filter, rough vacuum, DPL	1.62E-07	162	3.97E+05	397
9	**A**	**N**	26	5	2.00E-05	first flashover pic, filter too weak, DPR, **GOOD**	3.10E-07	310	4.49E+05	449
10	**A**	**N**	26	5	1.50E-05	filter too strong, DPL	1.46E-07	146	5.36E+05	536
11	**A**	**N**	26	5	2.00E-05	no pic, camera broke, DPR	2.98E-07	298	4.49E+05	449
12	**A**	**N**	26	5	1.70E-05	filter too strong, **load voltage,**	1.52E-07	152	1.64E+05	164
13	**A**	**N**	26	5	1.70E-05	filter too strong, DPL,	1.52E-07	152	1.73E+05	173
14	**A**	**N**	26	5	1.60E-05	filter too weak, **GOOD**	2.78E-07	278	1.99E+05	199
15	**A**	**N**	26	5	1.50E-05	filter too strong, large voltage spike,	2.66E-07	266	1.90E+05	190
16	**A**	**N**	26	5	1.50E-05	good pic, **GOOD**	2.88E-07	288	1.69E+05	169
17	**A**	**N**	34	8	1.50E-05	good pic, **GOOD**	2.62E-07	262	2.07E+05	207
18	**A**	**N**	40	11	1.40E-05	good pic, possible swingarm problem, **GOOD**	2.52E-07	252	2.87E+05	287
19	**A**	**N**	26	5	1.50E-05	**Possible No Flashover, GOOD**	5.00E-07	500	2.00E+05	200
20	**A**	**N**	26	5	1.40E-05	no data				
21	**A**	**N**	26	5	1.30E-05	no pic	3.05E-07	305	2.00E+05	200
22	**A**	**N**	28	5	1.20E-05		2.78E-07	278	2.25E+05	225
23	**A**	**N**	34	8	1.10E-05		2.69E-07	269	2.26E+05	226
24	**A**	**N**	34	8	1.10E-05		2.63E-07	263	2.78E+05	278
25	**A**	**N**	30	6	1.10E-05		2.57E-07	257	2.38E+05	238
26	**A**	**N**	30	6	1.10E-05		2.82E-07	282	2.35E+05	235
27	**A**	**N**	40	11	9.80E-06		2.89E-07	289	2.42E+05	242
28	**A**	**N**	40	11	9.80E-06		2.80E-07	280	2.71E+05	271
29	**A**	**N**	34	8	9.80E-06		2.72E-07	272	2.28E+05	228
30	**A**	**N**	34	8	9.80E-06		2.80E-07	280	2.35E+05	235
31	**A**	**N**	30	8	9.80E-06	bad oscope				
32	**A**	**N**	30	8	9.80E-06	bad oscope				
33	**A**	**N**	30	8	9.80E-06	bad oscope				
34	**A**	**N**	30	8	9.80E-06		2.73E-07	273	2.35E+05	235
35	**A**	**C**	26	5	1.70E-05	bad oscope				
36	**A**	**C**	26	5	1.70E-05	bad oscope				
37	**A**	**C**	26	5	1.60E-05		2.42E-07	242	1.69E+05	169
38	**A**	**C**	26	5	1.60E-05		2.34E-07	234	1.54E+05	154
39	**A**	**C**	34	8	1.50E-05		2.36E-07	236	2.11E+05	211
40	**A**	**C**	34	8	1.50E-05		2.44E-07	244	2.11E+05	211

Shot #	Insulator geometry	Shield type	Marx Charge (kV)	Marx Pressure (psig)	Chamber Pressure (Torr)	notes	Risetime 10-90%	Risetime (ns)	Max Voltage	Peak (kV)
41	**A**	**C**	34	8	1.50E-05		2.46E-07	246	2.07E+05	207
42	**A**	**C**	40	11	1.40E-05		2.36E-07	236	2.37E+05	237
43	**A**	**C**	40	11	1.40E-05		2.36E-07	236	2.54E+05	254
44	**A**	**C**	40	11	1.40E-05		2.40E-07	240	2.31E+05	231
45	**A**	**C**	30	7	1.40E-05		2.36E-07	236	1.81E+05	181
46	**A**	**C**	30	7	1.40E-05		2.30E-07	230	2.18E+05	218
47	**A**	**C**	30	7	1.30E-05		2.36E-07	236	1.90E+05	190
48	**A**	**C**	26	5	1.20E-05		2.42E-07	242	1.70E+05	170
49	**A**	**C**	26	5	1.20E-05		2.40E-07	240	1.92E+05	192
50	**A**	**C**	40	11	1.10E-05		2.28E-07	228	2.30E+05	230
51	**A**	**C**	40	11	1.10E-05		2.34E-07	234	2.45E+05	245
52	**A**	**C**	40	11	1.10E-05		2.34E-07	234	2.40E+05	240
53	**A**	**C**	34	8	1.10E-05		2.26E-07	226	2.25E+05	225
54	**A**	**C**	34	8	1.00E-05		2.34E-07	234	2.31E+05	231
55	**A**	**C**	45	13	1.00E-05		2.28E-07	228	2.75E+05	275
56	**A**	**C**	38	13	1.00E-05	Marx Prefire	2.26E-07	226	2.49E+05	249
57	**A**	**C**	34	8	1.00E-05		2.36E-07	236	2.04E+05	204
58	**A**	**C**	45	15	9.90E-06		2.30E-07	230	2.70E+05	270
59	**A**	**C**	38	15	9.90E-06	Marx Prefire	2.10E-07	210	1.93E+05	193
60	**A**	**C**	42	15	9.90E-06	Marx Prefire	1.92E-07	192	2.42E+05	242
61	**B**	**C**	26	5	1.40E-05	prefire, bad oscope settings				
62	**B**	**C**	26	5	1.40E-05	bad oscope				
63	**B**	**C**	26	5	1.40E-05	bad oscope				
64	**B**	**C**	26	5	1.10E-05	Dark Filter	2.36E-07	236	2.37E+05	237
65	**B**	**C**	26	5	1.00E-05	No Pic	1.78E-07	178	2.20E+05	220
66	**B**	**C**	26	5	9.80E-06	room light on	2.14E-07	214	2.40E+05	240
67	**B**	**C**	34	8	9.60E-06	prefire	1.64E-07	164	2.85E+05	285
68	**B**	**C**	34	9	9.40E-06	prefire	1.46E-07	146	2.76E+05	276
69	**B**	**C**	34	11	9.20E-06	prefire	2.20E-07	220	2.76E+05	276
70	**B**	**C**	38	13	9.00E-06	prefire	1.32E-07	132	2.59E+05	259
71	**B**	**C**	32	14	9.00E-06	prefire	1.54E-07	154	2.87E+05	287
72	**B**	**C**	30	14	8.80E-06		2.84E-07	284	2.88E+05	288
73	**B**	**C**	30	14	8.80E-06		2.20E-07	220	2.83E+05	283
74	**B**	**C**	30	13	8.70E-06		2.14E-07	214	2.69E+05	269
75	**B**	**C**	26	6	8.60E-06		2.00E-07	200	2.80E+05	280
76	**B**	**C**	26	6	8.50E-06		2.18E-07	218	2.66E+05	266
77	**B**	**C**	26	6	8.40E-06		2.20E-07	220	2.76E+05	276
78	**B**	**C**	40	15	8.30E-06		2.16E-07	216	3.11E+05	311
79	**B**	**C**	40	15	8.20E-06		2.20E-07	220	3.08E+05	308
80	**B**	**C**	40	15	8.10E-06	sounded weak	2.22E-07	222	2.97E+05	297
81	**B**	**C**	34	11	8.00E-06	sounded weak, similar data				
82	**B**	**C**	34	11	7.90E-06					
83	**B**	**C**	34	11	7.80E-06					
84	**B**	**C**	30	9	7.70E-06					

Shot #	Insulator geometry	Shield type	Marx Charge (kV)	Marx Pressure (psig)	Chamber Pressure (Torr)	notes	Risetime 10-90%	Risetime (ns)	Max Voltage	Peak (kV)
85	**B**	**C**	30	9	7.60E-06					
86	**B**	**C**	30	9	7.50E-06					
87	**B**	**N**	26	6	1.60E-05	no data				
88	**B**	**N**	26	6	1.60E-05	no data				
89	**B**	**N**	26	6	1.50E-05	no data				
90	**B**	**N**	34	11	1.50E-05		2.22E-07	222	2.78E+05	278
91	**B**	**N**	34	11	1.50E-05		2.12E-07	212	2.69E+05	269
92	**B**	**N**	34	11	1.40E-05	prefire, no pic, bad matlab	2.16E-07	216	2.63E+05	263
93	**B**	**N**	26	6	1.40E-05		2.28E-07	228	2.49E+05	249
94	**B**	**N**	26	6	1.30E-05		2.38E-07	238	2.49E+05	249
95	**B**	**N**	26	6	1.30E-05		2.16E-07	216	2.66E+05	266
96	**B**	**N**	39	15	1.20E-05	prefire	2.38E-07	238	2.97E+05	297
97	**B**	**N**	30	9	1.20E-05	no data				
98	**B**	**N**	26	9	1.20E-05	prefire	2.24E-07	224	2.52E+05	252
99	**B**	**N**	30	9	1.20E-05		2.18E-07	218	2.66E+05	266
100	**B**	**N**	30	9	1.20E-05		2.24E-07	224	2.80E+05	280
101	**B**	**N**	33	11	1.20E-05	prefire	2.20E-07	220	2.80E+05	280
102	**B**	**N**	34	13	1.20E-05		2.18E-07	218	2.90E+05	290
103	**B**	**N**	34	13	1.10E-05		2.22E-07	222	2.87E+05	287
104	**B**	**N**	40	16	1.10E-05		2.18E-07	218	3.04E+05	304
105	**B**	**N**	40	16	1.10E-05	sounded like arc in air	2.22E-07	222	3.08E+05	308
106	**B**	**N**	26	6	1.10E-05		2.20E-07	220	2.52E+05	252
107	**B**	**N**	26	6	1.00E-05		2.14E-07	214	2.69E+05	269
108	**B**	**N**	26	6	1.00E-05		2.22E-07	222	2.66E+05	266
109	**B**	**N**	30	9	1.00E-05		2.26E-07	226	2.76E+05	276
110	**B**	**N**	30	9	1.00E-05		2.16E-07	216	2.66E+05	266
111	**B**	**N**	30	9	1.00E-05		2.18E-07	218	2.80E+05	280
112	**B**	**N**	26	5		**sandia vistors**				
113	**B**	**N**	26	5		sandia vistors				
114	**B**	**N**	26	5		sandia vistors				
115	**B**	**N**	26	5		sandia vistors				
116	**C**	**N**	32	5	1.50E-05		1.92E-07	192	2.11E+05	211
117	**C**	**N**	36	5	1.50E-05	no data, bottom flashover				
118	**C**	**N**	36	5	1.50E-05	bottom flashover	1.92E-07	192	2.11E+05	211
119	**C**	**N**	36	5	5.00E-02	sanded bottom, rough pump only	2.20E-07	220	2.28E+05	228
120	**C**	**N**	36	5	5.00E-02	rough pump only	2.22E-07	222	2.49E+05	249
121	**C**	**N**	36	5	5.00E-02	rough pump only	2.14E-07	214	2.69E+05	269
122	**C**	**N**	36	5	5.00E-02	rough pump only	1.93E-07	193	2.90E+05	290
123	**C**	**N**	36	5	5.00E-02	rough pump only	2.09E-07	209	2.69E+05	269
124	**C**	**N**	36	5	5.00E-02	rough pump only	1.83E-07	183	2.90E+05	290
125	**C**	**N**	36	5	5.00E-02	rough pump only	1.85E-07	185	2.87E+05	287
126	**C**	**N**	36	5	1.20E-05	full vacuum	2.19E-07	219	2.66E+05	266
127	**C**	**N**	36	5	1.20E-05		2.06E-07	206	2.90E+05	290
128	**C**	**N**	36	5	1.20E-05		1.76E-07	176	2.87E+05	287

Shot #	Insulator geometry	Shield type	Marx Charge (kV)	Marx Pressure (psig)	Chamber Pressure (Torr)	notes	Risetime 10-90%	Risetime (ns)	Max Voltage	Peak (kV)
129	**C**	**N**	36	5	1.20E-05		2.28E-07	228	2.69E+05	269
130	**C**	**C**	36	5	1.20E-05		2.37E-07	237	1.17E+05	117
131	**C**	**C**	36	5	1.20E-05		2.18E-07	218	1.24E+05	124
132	**C**	**C**	36	5	1.20E-05		2.13E-07	213	1.38E+05	138
133	**C**	**C**	36	5	1.20E-05		2.14E-07	214	1.31E+05	131
134	**C**	**C**	36	5	1.20E-05			0		
135	**C**	**C**	36	5	1.20E-05		2.13E-07	213	1.31E+05	131
136	**C**	**C**	34	5	1.20E-05	prefire	2.24E-07	224	1.24E+05	124
137	**C**	**C**	38	5	1.20E-05	prefire	2.20E-07	220	1.21E+05	121
138	**C**	**C**	40	5	1.20E-05		2.24E-07	224	1.35E+05	135
139	**C**	**C**	40	5	1.20E-05		2.46E-07	246	1.31E+05	131
140	**C**	**C**	40	5	1.20E-05		2.26E-07	226	1.31E+05	131
141	**D**	**N**	36	6	1.00E-05		2.14E-07	214	3.14E+05	314
142	**D**	**N**	36	6	1.00E-05		2.14E-07	214	3.45E+05	345
143	**D**	**N**	38	6	1.00E-05		2.11E-07	211	3.49E+05	349
144	**D**	**N**	36	6	1.00E-05		2.10E-07	210	3.08E+05	308
145	**D**	**N**	36	6	1.00E-05		1.94E-07	194	3.35E+05	335
146	**D**	**N**	40	12	1.00E-05		2.11E-07	211	3.90E+05	390
147	**D**	**N**	40	12	1.00E-05		2.08E-07	208	3.49E+05	349
148	**D**	**N**	40	12	1.00E-05		2.07E-07	207	3.63E+05	363
149	**D**	**N**	44	14	1.00E-05		2.16E-07	216	3.56E+05	356
150	**D**	**N**	44	14	1.00E-05		2.11E-07	211	3.90E+05	390
151	**E**	**A**	36	10	8.00E-06	Dark filter	2.29E-07	229	6.18E+05	618
152	**E**	**A**	36	10	8.00E-06	no filter	2.66E-07	266	5.56E+05	556
153	**E**	**A**	36	10	8.00E-06	dark filter	2.59E-07	259	4.84E+05	484
154	**E**	**A**	36	10	8.00E-06	Dark filter	2.59E-07	259	4.80E+05	480
155	**E**	**A**	40	12	8.00E-06	Purged no filter	2.30E-07	230	5.36E+05	536
156	**E**	**A**	38	12	8.00E-06	selfbreak, no pic	2.32E-07	232	5.84E+05	584
157	**E**	**A**	40	13	8.00E-06	no pic	2.18E-07	218	5.98E+05	598
158	**E**	**A**	40	13	8.00E-06	room light on	2.20E-07	220	5.29E+05	529
159	**E**	**A**	40	17	8.00E-06	selfbreak, no pic	2.20E-07	220	5.29E+05	529
160	**E**	**A**	36	19	8.00E-06	selfbreak, no pic	2.24E-07	224	5.11E+05	511
161	**E**	**A**	44	21	8.00E-06	no pic	2.23E-07	223	5.91E+05	591
162	**E**	**A**	44	22	8.00E-06	selfbreak, no pic	2.18E-07	218	5.87E+05	587
163	**E**	**A**	34	13	8.00E-06		2.23E-07	223	4.01E+05	401
164	**E**	**A**	40	18	8.00E-06		2.24E-07	224	4.91E+05	491
165	**E**	**A**	36	15	8.00E-06		2.19E-07	219	4.80E+05	480
166	**E**	**AC**	36	11	8.00E-06	prefire	2.39E-07	239	4.73E+05	473
167	**E**	**AC**	36	14	8.00E-06		2.32E-07	232	3.94E+05	394
168	**E**	**AC**	36	14	8.00E-06		2.28E-07	228	4.70E+05	470
169	**E**	**AC**	36	14	8.00E-06		2.23E-07	223	4.63E+05	463
170	**E**	**AC**	40	18	8.00E-06		2.22E-07	222	4.77E+05	477
171	**E**	**AC**	40	18	8.00E-06		2.39E-07	239	4.87E+05	487
172	**E**	**AC**	40	18	8.00E-06		2.21E-07	221	5.04E+05	504

Shot #	Insulator geometry	Shield type	Marx Charge (kV)	Marx Pressure (psig)	Chamber Pressure (Torr)	notes	Risetime 10-90%	Risetime (ns)	Max Voltage	Peak (kV)
173	**E**	**AC**	40	18	8.00E-06		2.25E-07	225	5.36E+05	536
174	**E**	**AC**	44	22	8.00E-06	prefire	2.33E-07	233	6.05E+05	605
175	**E**	**AC**	44	23	8.00E-06		2.28E-07	228	5.39E+05	539
176	**E**	**AC**	44	23	8.00E-06		2.25E-07	225	5.63E+05	563
177	**E**	**AC**	40	23	8.00E-06	selfbreak, no pic	1.92E-07	192	4.66E+05	466
178	**E**	**AC**	44	25	8.00E-06		2.26E-07	226	5.74E+05	574
179	**D**	**N**	36	13	8.00E-06	possible flashover on bottom	1.67E-07	167	6.18E+05	618
180	**D**	**N**	36	13	8.00E-06	possible flashover on bottom	1.72E-07	172	6.18E+05	618
181	**D**	**N**	36	13	8.00E-06	possible flashover on bottom	1.70E-07	170	9.33E+05	933
182	**D**	**N**	36	13	8.00E-06	possible flashover on bottom	1.86E-07	186	1.10E+06	1100
183	**D**	**N**	36	13	8.00E-06	flashover on bottom	1.90E-07	190	8.98E+05	898
184	**D**	**N**	36	13	8.00E-06	flashover on bottom	1.88E-07	188	9.93E+05	993
185	**D**	**N**	36	13	8.00E-06	flashover on bottom	1.97E-07	197	1.09E+06	1090
186	**D**	**N**	36	13	8.00E-06	first shot with chamber anode field shaper	1.90E-07	190	8.55E+05	855
187	**D**	**N**	36	13	8.00E-06		1.75E-07	175	6.65E+05	665
188	**D**	**N**	36	13	8.00E-06		1.83E-07	183	8.12E+05	812
189	**F**	**N**	36	13	6.00E-06	2 time atten.	2.43E-07	243	1.30E+05	130
190	**F**	**N**	34	13	6.00E-06	S.B. No Pic	2.37E-07	237	2.59E+05	259
191	**F**	**N**	40	18	6.00E-06		2.28E-07	228	2.45E+05	245
192	**F**	**N**	40	18	6.00E-06		2.27E-07	227	2.42E+05	242
193	**F**	**N**	44	23	6.00E-06		2.35E-07	235	2.76E+05	276
194	**F**	**N**	44	23	6.00E-06		2.32E-07	232	2.66E+05	266
195	**F**	**N**	36	13	6.00E-06		2.37E-07	237	2.14E+05	214
196	**F**	**N**	36	13	6.00E-06		2.39E-07	239	2.07E+05	207
197	**F**	**N**	40	18	6.00E-06		2.27E-07	227	2.38E+05	238
198	**F**	**N**	40	18	6.00E-06		2.39E-07	239	2.21E+05	221
199	**F**	**N**	44	25	6.00E-06		2.33E-07	233	2.76E+05	276
200	**F**	**N**	44	25	6.00E-06		2.35E-07	235	2.52E+05	252
						Zero Degree no shield summary	2.34E-07	234	2.36E+05	236
202	**F**	**C**	36	13	6.00E-06		2.49E-07	249	1.76E+05	176
203	**F**	**C**	36	14	6.00E-06		2.30E-07	230	2.07E+05	207
204	**F**	**C**	40	19	6.00E-06		2.50E-07	250	1.90E+05	190
205	**F**	**C**	40	19	6.00E-06		2.72E-07	272	1.87E+05	187
206	**F**	**C**	40	24	6.00E-06		2.40E-07	240	2.04E+05	204
207	**F**	**C**	42	24	6.00E-06		2.44E-07	244	2.07E+05	207
208	**F**	**C**	44	25	6.00E-06		2.40E-07	240	2.31E+05	231
209	**F**	**C**	44	25	6.00E-06		2.34E-07	234	2.56E+05	256
210	**F**	**C**	40	10	6.00E-06		2.36E-07	236	2.35E+05	235
211	**F**	**C**	40	25	6.00E-06	SB No Pic	2.76E-07	276	1.97E+05	197
212	**F**	**C**	44	25	6.00E-06		2.37E-07	237	2.56E+05	256
213	**F**	**C**	36	14	6.00E-06		2.39E-07	239	2.07E+05	207
214	**F**	**C**	38	14	6.00E-06		2.41E-07	241	2.25E+05	225
						zero degree cathode shield summary	2.45E-07	2.45E+02	2.14E+05	2.14E+02
215	**F**	**A**	36	13	6.00E-06		2.36E-07	236	1.80E+05	180
216	**F**	**A**	36	13	6.00E-06		2.37E-07	237	1.90E+05	190

Shot #	Insulator geometry	Shield type	Marx Charge (kV)	Marx Pressure (psig)	Chamber Pressure (Torr)	notes	Risetime 10-90%	Risetime (ns)	Max Voltage	Peak (kV)
217	**F**	**A**	40	19	6.00E-06		2.33E-07	233	2.18E+05	218
218	**F**	**A**	36	18	6.00E-06	SB	2.00E-07	200	2.25E+05	225
219	**F**	**A**	40	19	6.00E-06		2.38E-07	238	2.38E+05	238
220	**F**	**A**	44	25	6.00E-06		2.38E-07	238	2.28E+05	228
221	**F**	**A**	44	25	6.00E-06		2.38E-07	238	2.49E+05	249
222	**F**	**A**	40	19	6.00E-06	SB	2.42E-07	242	2.00E+05	200
223	**F**	**A**	44	25	6.00E-06		2.41E-07	241	2.45E+05	245
224	**F**	**A**	44	25	6.00E-06		2.40E-07	240	2.73E+05	273
225	**F**	**A**	40	19	6.00E-06	SB	1.93E-07	193	2.83E+05	283
226	**F**	**A**	36	15	6.00E-06		2.37E-07	237	2.31E+05	231
						zero degree anode shield summary	2.31E-07	2.31E+02	2.30E+05	2.30E+02
227	**F**	**AC**	36	15	6.00E-06		2.36E-07	236	1.90E+05	190
228	**F**	**AC**	36	15	6.00E-06		2.33E-07	233	2.18E+05	218
229	**F**	**AC**	40	20	6.00E-06		2.34E-07	234	2.18E+05	218
230	**F**	**AC**	40	20	6.00E-06		2.38E-07	238	2.35E+05	235
231	**F**	**AC**	44	25	6.00E-06		2.36E-07	236	2.42E+05	242
232	**F**	**AC**	44	25	6.00E-06		2.45E-07	245	2.38E+05	238
233	**F**	**AC**	32	20	6.00E-06	SB	2.26E-07	226	2.11E+05	211
234	**F**	**AC**	40	20	6.00E-06		2.39E-07	239	2.31E+05	231
235	**F**	**AC**	40	20	6.00E-06		2.37E-07	237	2.28E+05	228
236	**F**	**AC**	44	24	6.00E-06	SB	2.75E-07	275	2.21E+05	221
237	**F**	**AC**	44	25	6.00E-06		2.41E-07	241	2.56E+05	256
238	**F**	**AC**	36	15	6.00E-06		2.45E-07	245	2.28E+05	228
239	**F**	**AC**	36	15	6.00E-06		3.02E-07	302	1.93E+05	193
						zero degree both shield summary	2.45E-07	2.45E+02	2.24E+05	2.24E+02
240	**G**	**N**	32	20	6.00E-06	Flash on bottom of chamber				
241	**G**	**N**	32	20	6.00E-06	Flash on bottom of chamber				
242	**G**	**N**	32	20	6.00E-06	Flash on bottom of chamber				
243	**G**	**N**	32	20	6.00E-06	Flash on bottom of chamber				
244	**G**	**N**	32	20	6.00E-06	Flash on bottom of chamber				
245	**G**	**N**	32	20	6.00E-06	Flash on bottom of chamber				
246	**G**	**N**	32	20	6.00E-06	Flash on bottom of chamber				
247	**G**	**N**	32	20	6.00E-06	Flash on bottom of chamber				
248	**G**	**N**	32	20	6.00E-06	Flash on bottom of chamber				
249	**G**	**N**	32	20	6.00E-06	Flash on bottom of chamber				
250	**G**	**N**	32	20	6.00E-06	Flash on bottom of chamber				
251	**G**	**N**	32	20	6.00E-06	Flash on bottom of chamber				
252	**G**	**N**	32	20	6.00E-06	Flash on bottom of chamber				
253	**G**	**A**	32	20	7.00E-06	Flash on bottom of chamber				
254	**G**	**A**	32	20	7.00E-06	Flash on bottom of chamber				
255	**G**	**A**	32	20	7.00E-06	Flash on bottom of chamber				
256	**G**	**A**	32	20	7.00E-06	Flash on bottom of chamber				
257	**G**	**A**	32	20	7.00E-06	Flash on bottom of chamber				
258	**G**	**C**	32	20	6.00E-06	OK				
259	**G**	**C**	32	20	6.00E-06	OK				
260	**G**	**C**	32	20	6.00E-06	OK				

Shot #	Insulator geometry	Shield type	Marx Charge (kV)	Marx Pressure (psig)	Chamber Pressure (Torr)	notes	Risetime 10-90%	Risetime (ns)	Max Voltage	Peak (kV)
261	**G**	**C**	32	20	6.00E-06	OK				
262	**G**	**C**	32	20	6.00E-06	OK				
263	**G**	**C**	32	20	6.00E-06	OK				
264	**G**	**AC**	32	20	8.50E-06	OK				
265	**G**	**AC**	32	20	8.50E-06	OK				
266	**G**	**AC**	32	20	8.50E-06	OK				
267	**G**	**AC**	32	20	8.50E-06	OK				
268	**G**	**AC**	32	20	8.50E-06	OK				
269	**G**	**AC**	32	20	8.50E-06	OK				
270	**G**	**AC**	32	20	8.50E-06	OK				
271	**G**	**N**	32	20	9.00E-06	Flashover on bottom of chamber				
272	**G**	**N**	32	20	9.00E-06	Flashover on bottom of chamber				
273	**G**	**N**	32	20	9.00E-06	Flashover on bottom of chamber				
274	**G**	**N**	32	20	9.00E-06	Flashover on bottom of chamber				
275	**G**	**N**	32	20	9.00E-06	Flashover on bottom of chamber				
276	**G**	**N**	32	20	9.00E-06	Flashover on bottom of chamber				
277	**G**	**N**	32	20	9.00E-06	Flashover on bottom of chamber				
278	**G**	**N**	32	20	9.00E-06	Flashover on bottom of chamber				
279	**G**	**N**	32	20	9.00E-06	Flashover on bottom of chamber				
280	**G**	**N**	32	20	9.00E-06	Flashover on bottom of chamber				
281	**G**	**N**	32	20	9.00E-06	Flashover on bottom of chamber				
282	**G**	**N**	32	20	9.00E-06	Flashover on bottom of chamber				
283	**G**	**N**	32	20	9.00E-06	Flashover on bottom of chamber				
284	**G**	**N**	32	20	9.00E-06	Flashover on bottom of chamber				
285	**G**	**N**	32	20	9.00E-06	Flashover on bottom of chamber				
286	**G**	**N**	32	20	9.00E-06	Flashover on bottom of chamber				
287	**G**	**N**	32	20	9.00E-06	Flashover on bottom of chamber				
288	**G**	**N**	32	20	9.00E-06	Flashover on bottom of chamber				
289	**G**	**N**	32	20	9.00E-06	Flashover on bottom of chamber				
290	**G**	**N**	32	20	9.00E-06	Flashover on bottom of chamber				
291	**G**	**N**	32	20	9.00E-06	Flashover on bottom of chamber				
292	**G**	**N**	32	20	9.00E-06	Flashover on bottom of chamber				
293	**G**	**N**	32	20	9.00E-06	Flashover on bottom of chamber				
294	**G**	**N**	32	20	9.00E-06	Flashover on bottom of chamber				
295	**G**	**N**	32	20	9.00E-06	Flashover on bottom of chamber				
296	**G**	**N**	32	20	9.00E-06	Flashover on bottom of chamber				
297	**G**	**N**	32	20	9.00E-06	Flashover on bottom of chamber				
298	**G**	**N**	32	20	9.00E-06	Flashover on bottom of chamber				
299	**G**	**N**	32	20	9.00E-06	Flashover on bottom of chamber				
300	**G**	**N**	32	20	9.00E-06	Installing high speed camera				
301	**G**	**N**	32	20	9.00E-06	Installing high speed camera				
302	**G**	**N**	32	20	9.00E-06	Installing high speed camera				
303	**G**	**N**	32	20	9.00E-06	Installing high speed camera				
304	**G**	**N**	32	20	9.00E-06	Installing high speed camera				

Shot #	Insulator geometry	Shield type	Marx Charge (kV)	Marx Pressure (psig)	Chamber Pressure (Torr)	notes	Risetime 10-90%	Risetime (ns)	Max Voltage	Peak (kV)
305	**G**	**N**	32	20	9.00E-06	Installing high speed camera				
306	**G**	**N**	32	20	9.00E-06	Installing high speed camera				
307	**G**	**C**	32	20	6.00E-06	started statistical format			3.29E+05	329
308	**G**	**C**	32	20	6.00E-06	Framing camera (FC) 8us per image			3.59E+05	359
309	**G**	**C**	32	20	6.00E-06	marx self broke			3.74E+05	374
310	**G**	**C**	32	20	6.00E-06	No FC			3.79E+05	379
311	**G**	**C**	32	20	6.00E-06	FC 8us			4.04E+05	404
312	**G**	**C**	32	20	6.00E-06	FC 4us			3.30E+05	330
313	**G**	**C**	32	20	6.00E-06	FC 2 us			3.59E+05	359
314	**G**	**C**	32	20	6.00E-06	FC 1:3us(2,3,4:1us) 7:3us(6,5,8:1us)			3.74E+05	374
315	**G**	**C**	32	20	6.00E-06	FC 1:3us(2,3,4:1us) 7:3us(6,5,8:1us)			3.78E+05	378
316	**G**	**C**	32	20	6.00E-06	FC 500ns all stepped			3.16E+05	316
317	**G**	**C**	32	20	6.00E-06	FC 500ns all stepped			3.29E+05	329
318	**G**	**C**	32	20	6.00E-06	FC 500ns all stepped			3.59E+05	359
319	**G**	**C**	32	20	6.00E-06	FC 500ns all stepped			3.19E+05	319
320	**G**	**C**	32	20	6.00E-06	FC 500ns all stepped			3.59E+05	359
321	**G**	**C**	32	20	6.00E-06	FC 500ns all stepped			3.59E+05	359
						summary 45 cathode shield				**355**
322	**G**	**A**	32	20	5.00E-06	FC 1:3us(2,3,4:1us) 7:3us(6,5,8:1us)			3.37E+05	337
323	**G**	**A**	32	20	5.00E-06	FC 2 us stepped			3.37E+05	337
324	**G**	**A**	32	20	5.00E-06	FC 4us stepped			3.49E+05	349
325	**G**	**A**	32	20	5.00E-06	FC 1.5us 4.5 us envelope			3.62E+05	362
326	**G**	**A**	32	20	5.00E-06	FC 1.5us 4.5 us envelope			3.37E+05	337
327	**G**	**A**	32	20	5.00E-06	4 us step			3.12E+05	312
328	**G**	**A**	32	20	5.00E-06	2 us step			3.12E+05	312
329	**G**	**A**	32	20	5.00E-06	2 us stepd (no good off center)			3.72E+05	372
330	**G**	**A**	32	20	5.00E-06	2 us step			3.49E+05	349
331	**G**	**A**	32	20	5.00E-06	marx self break			3.12E+05	312
332	**G**	**A**	32	20	5.00E-06	marx self break			3.71E+05	371
333	**G**	**A**	32	20	5.00E-06	10 us step			3.72E+05	372
334	**G**	**A**	32	20	5.00E-06	FC 1.5 us step with 4.5 us envelope			3.13E+05	313
335	**G**	**A**	32	20	5.00E-06	FC 1 us step with 3 us envelope			3.12E+05	312
336	**G**	**A**	32	20	5.00E-06	800 ns step with 2.4 us envelope			3.11E+05	311
337	**G**	**A**	32	20	5.00E-06	800 ns step with 2.4 us envelope			3.11E+05	311
						summary 45 anode shield				**335**
338	**G**	**N**	32	20	4.50E-06	FC stopped working reliably				
339	**G**	**N**	32	20	4.50E-06	OK			3.00E+05	300
340	**G**	**N**	32	20	4.50E-06	OK			2.87E+05	287
341	**G**	**N**	32	20	4.50E-06	OK			3.12E+05	312
342	**G**	**N**	32	20	4.50E-06	OK			3.50E+05	350
343	**G**	**N**	32	20	4.50E-06				3.00E+05	300
344	**G**	**N**	32	20	4.50E-06				2.87E+05	287
345	**G**	**N**	32	20	4.50E-06				3.12E+05	312
346	**G**	**N**	32	20	4.50E-06				2.87E+05	287
347	**G**	**N**	32	20	4.50E-06				3.12E+05	312
348	**G**	**N**	32	20	4.50E-06				2.87E+05	287

Shot #	Insulator geometry	Shield type	Marx Charge (kV)	Marx Pressure (psig)	Chamber Pressure (Torr)	notes	Risetime 10-90%	Risetime (ns)	Max Voltage	Peak (kV)
349	**G**	**N**	32	20	4.50E-06				2.87E+05	287
350	**G**	**N**	32	20	4.50E-06				3.25E+05	325
351	**G**	**N**	32	20	4.50E-06				3.12E+05	312
352	**G**	**N**	32	20	4.50E-06					
						summary 45 no shield				**305**
353	**G**	**AC**	32	20	4.70E-06	ok			2.72E+05	272
354	**G**	**AC**	32	20	4.70E-06				2.72E+05	272
355	**G**	**AC**	32	20	4.70E-06	used roxbox to trigger marx			2.50E+05	250
356	**G**	**AC**	32	20	4.70E-06				2.86E+05	286
357	**G**	**AC**	32	20	4.70E-06				2.74E+05	274
358	**G**	**AC**	32	20	4.70E-06				2.72E+05	272
359	**G**	**AC**	32	20	4.70E-06				2.86E+05	286
360	**G**	**AC**	32	20	4.70E-06				3.22E+05	322
361	**G**	**AC**	32	20	4.70E-06				2.72E+05	272
362	**G**	**AC**	32	20	4.70E-06				2.50E+05	250
363	**G**	**AC**	32	20	4.70E-06				2.72E+05	272
364	**G**	**AC**	32	20	4.70E-06				2.86E+05	286
365	**G**	**AC**	32	20	4.70E-06	louder than usual				
366	**G**	**AC**	32	20	4.70E-06				2.99E+05	299
367	**G**	**AC**	32	20	4.70E-06				2.72E+05	272
368	**G**	**AC**	32	20	4.70E-06				2.99E+05	299
						summary 45 cathode and anode shield				**280**
369	**F**	**N**	32	20	4.70E-06	Framing camera still not working				
370	**F**	**N**	32	20	4.70E-06				2.19E+05	219
371	**F**	**N**	32	20	4.70E-06	quieter			2.55E+05	255
372	**F**	**N**	32	20	4.70E-06				2.19E+05	219
373	**F**	**N**	32	20	4.70E-06				2.70E+05	270
374	**F**	**N**	32	20	4.70E-06				2.19E+05	219
375	**F**	**N**	32	20	4.70E-06				1.57E+05	157
376	**F**	**N**	32	20	4.70E-06				2.32E+05	232
377	**F**	**N**	32	20	4.70E-06				2.19E+05	219
378	**F**	**N**	32	20	4.70E-06				2.32E+05	232
379	**F**	**N**	32	20	4.70E-06				2.55E+05	255
380	**F**	**N**	32	20	4.70E-06					
381	**F**	**N**	32	20	4.70E-06				2.19E+05	219
382	**F**	**N**	32	20	4.70E-06				1.57E+05	157
383	**F**	**N**	32	20	4.70E-06				2.32E+05	232
						summary zero no shield				**222**
384	**G**	**N**	32	20	5.00E-06	framing camera still not working			2.87E+05	287
385	**G**	**N**	32	20	5.00E-06				3.12E+05	312
386	**G**	**N**	32	20	5.00E-06				3.25E+05	325
387	**G**	**N**	32	20	5.00E-06				2.87E+05	287
388	**G**	**N**	32	20	5.00E-06				3.12E+05	312
389	**G**	**N**	32	20	5.00E-06				3.12E+05	312
390	**G**	**N**	32	20	5.00E-06				3.12E+05	312
391	**G**	**N**	32	20	5.00E-06	Loud noise from I-store			3.00E+05	300
392	**G**	**N**	32	20	5.00E-06	ok			3.12E+05	312

Shot #	Insulator geometry	Shield type	Marx Charge (kV)	Marx Pressure (psig)	Chamber Pressure (Torr)	notes	Risetime 10-90%	Risetime (ns)	Max Voltage	Peak (kV)
393	**G**	**N**	32	20	5.00E-06				3.12E+05	312
394	**G**	**N**	32	20	5.00E-06				3.25E+05	325
395	**G**	**N**	32	20	5.00E-06				2.87E+05	287
396	**G**	**N**	32	20	5.00E-06				3.50E+05	350
397	**G**	**N**	32	20	5.00E-06				3.25E+05	325
398	**G**	**N**	32	20	5.00E-06				3.00E+05	300
399	**G**	**N**	32	20	5.00E-06	self break				
						summary 45 no shield				**312**
400	**G**	**CA**	32	20	5.00E-06	file 400 corrupted data in '400a'			2.72E+05	272
401	**G**	**CA**	32	20	5.00E-06	ok			3.22E+05	322
402	**G**	**CA**	32	20	5.00E-06				2.86E+05	286
403	**G**	**CA**	32	20	5.00E-06				2.86E+05	286
404	**G**	**CA**	32	20	5.00E-06				3.50E+05	350
405	**G**	**CA**	32	20	5.00E-06				3.22E+05	322
406	**G**	**CA**	32	20	5.00E-06				2.86E+05	286
407	**G**	**CA**	32	20	5.00E-06				2.72E+05	272
408	**G**	**CA**	32	20	5.00E-06				2.72E+05	272
409	**G**	**CA**	32	20	5.00E-06				2.50E+05	250
410	**G**	**CA**	32	20	5.00E-06				2.72E+05	272
411	**G**	**CA**	32	20	5.00E-06				2.99E+05	299
412	**G**	**CA**	32	20	5.00E-06				3.12E+05	312
413	**G**	**CA**	32	20	5.00E-06				2.86E+05	286
414	**G**	**CA**	32	20	5.00E-06				2.72E+05	272
						summary 45 cathode and anode shield				**291**
415	**F**	**N**	32	20	6.50E-06	ok				
416	**F**	**N**	32	20	6.50E-06				2.19E+05	219
417	**F**	**N**	32	20	6.50E-06				2.70E+05	270
418	**F**	**N**	32	20	6.50E-06				2.32E+05	232
419	**F**	**N**	32	20	6.50E-06				2.32E+05	232
420	**F**	**N**	32	20	6.50E-06				2.43E+05	243
421	**F**	**N**	32	20	6.50E-06				2.32E+05	232
422	**F**	**N**	32	20	6.50E-06				2.55E+05	255
423	**F**	**N**	32	20	6.50E-06					
424	**F**	**N**	32	20	6.50E-06				2.32E+05	232
425	**F**	**N**	32	20	6.50E-06				2.55E+05	255
426	**F**	**N**	32	20	6.50E-06				2.32E+05	232
427	**F**	**N**	32	20	6.50E-06				2.43E+05	243
428	**F**	**N**	32	20	6.50E-06					
429	**F**	**N**	32	20	6.50E-06					
						summary zero no shield				**241**
430	**G**	**N**	32	20	5.00E-06	Forgot shield had to open chamber				
431	**G**	**C**	32	20	5.00E-06	ok			3.59E+05	359
432	**G**	**C**	32	20	5.00E-06				3.19E+05	319
433	**G**	**C**	32	20	5.00E-06				3.44E+05	344
434	**G**	**C**	32	20	5.00E-06				3.80E+05	380
435	**G**	**C**	32	20	5.00E-06				3.54E+05	354
436	**G**	**C**	32	20	5.00E-06				3.44E+05	344

Shot #	Insulator geometry	Shield type	Marx Charge (kV)	Marx Pressure (psig)	Chamber Pressure (Torr)	notes	Risetime 10-90%	Risetime (ns)	Max Voltage	Peak (kV)
437	**G**	**C**	32	20	5.00E-06				3.29E+05	329
438	**G**	**C**	32	20	5.00E-06	marx self broke			3.55E+05	355
439	**G**	**C**	32	20	5.00E-06				3.30E+05	330
440	**G**	**C**	32	20	5.00E-06				3.78E+05	378
441	**G**	**C**	32	20	5.00E-06				4.04E+05	404
442	**G**	**C**	32	20	5.00E-06				3.29E+05	329
443	**G**	**C**	32	20	5.00E-06				3.16E+05	316
444	**G**	**C**	32	20	5.00E-06				3.16E+05	316
445	**G**	**C**	32	20	5.00E-06				3.17E+05	317
						summary 45 cathode shield				**345**
446	**G**	**A**	32	20	5.00E-06	ok			3.71E+05	371
447	**G**	**A**	32	20	5.00E-06				3.49E+05	349
448	**G**	**A**	32	20	5.00E-06				3.62E+05	362
449	**G**	**A**	32	20	5.00E-06				3.37E+05	337
450	**G**	**A**	32	20	5.00E-06				3.12E+05	312
451	**G**	**A**	32	20	5.00E-06				3.12E+05	312
452	**G**	**A**	32	20	5.00E-06				3.37E+05	337
						summary 45 anode shield				**341**

Appendix B: Matlab Script

```
%shot number
SN='AB1'

%raw data
[labels,marxcurrent_time,marxcurrentraw]=readColData(['shot',SN,'-9.txt'],2,1,1);
[labels,loadvoltage_time,loadvoltageraw]=readColData(['shot',SN,'-11.txt'],2,1,1);

%with 2X atten
marxcurrent=marxcurrentraw*6330.330330;
loadvoltage=loadvoltageraw*1220*17.7*2*.8795;

[marxcurrentfiltered,dt]=butterfilterupdated2(marxcurrent_time,marxcurrent,1e7,20,300,
299);
[loadvoltagefiltered,dt]=butterfilterupdated2(loadvoltage_time,loadvoltage,1e7,20,300,29
9);

plot(marxcurrent_time,marxcurrent,'y')
plot(loadvoltage_time,loadvoltage,'r')

tr=risetime(loadvoltage_time,loadvoltagefiltered)
teff=teffective(loadvoltage_time,loadvoltagefiltered)
flashV=max(abs(loadvoltage))

function tr = risetime(t, y);
% tr = risetime(t, y) returns the rise time of a response y
% i.e., the time from 10% to 90% of the
% final value in y. Time is in vector t.
final = max(abs(y)); %get highest value of magnitude of y in data
% (risetime will not work if system does not reach
% steady state)
index = 0;
finalcheck = 0;
while finalcheck < final
   index = index + 1;
   finalcheck=abs(y(index));
end

%tenper = find(abs(y) >= 0.1*final); % find returns the indices of y which
% are at least 10% of the final value
ninetyper=final;
while ninetyper>0.9*final
   ninetyper=abs(y(index));
   index=index-1;
end
```

```
ninetyperindex=index
tenper=abs(ninetyper);
while tenper>0.1*final
   tenper=abs(y(index));
   index=index-1;
end;
tenperindex=index
tr=t(ninetyperindex)-t(tenperindex);
%ninetyper = find(abs(y) >= 0.9*final); % find indices of y which are at least
% 90% of the final value
%tr = t(ninetyper(1)) - t(tenper(1)); % rise time is difference between the
% first crossing of 10% and of 90%

function teff = teffective(t, y);
% tr = teff(t, y) returns the t effective time of a response y
% i.e., the time from 63% to max of y

final = max(abs(y)); %get highest value of magnitude of y in data

index = 0;
finalcheck = 0;
while finalcheck < final
   index = index + 1;
   finalcheck=abs(y(index));
end
finalcheckindex=index;

teffvoltage=final;
while teffvoltage>0.63*final
   teffvoltage=abs(y(index));
   index=index-1;
end
teffvoltageindex=index;

teff=t(finalcheckindex)-t(teffvoltageindex);
```

References

[1] W. A. Stygar, J. A. Lott, T. C. Wagoner, V. Anaya, H. C. Harjes, H. C. Ives, Z. R. Wallace, G. R. Mowrer, R. W. Shoup, J. P. Corley, R. A. Anderson, G. E. Vogtlin, M. E. Savage, J. M. Elizondo, B. S. Stoltzfus, D. M. Andercyk, D. L. Fehl, T. F. Jaramillo, D. L. Johnson, D. H. McDaniel, D. A. Muirhead, J. M. Radman, J. J. Ramirez, L. E. Ramirez, R. B. Spielman, K. W. Struve, and D. E. Walsh, "Improved design of a high-voltage vacuum-insulator interface," *Phys. Rev. ST Accel. Beams*, vol. 8, no. 5, p. 050401, May2005.

[2] J. M. Elizondo, K. Struve, B. Stygar, and K. Prestwich, "Vacuum flashover characteristics of solid CL-polystyrene," 2002, pp. 650-653.

[3] I. D. Smith, P. A. Corcoran, W. A. Stygar, T. H. Martin, R. B. Spielman, and R. W. Shoup, "Design criteria for the Z vacuum insulator stack,", 1 ed 1997, pp. 168-176.

[4] E. A. Weinbrecht, D. H. McDaniel, and D. D. Bloomquist, "The Z refurbishment project (ZR) at Sandia National Laboratories,", 1 ed 2003, pp. 157-162.

[5] W. A. Stygar, H. C. Ives, T. C. Wagoner, J. A. Lott, V. Anaya, H. C. Harjes, J. P. Corley, R. W. Shoup, D. L. Fehl, G. R. Mowrer, Z. R. Wallace, R. A. Anderson, J. D. Boyes, J. W. Douglas, M. L. Horry, T. F. Jaramillo, D. L. Johnson, F. W. Long, T. H. Martin, D. H. McDaniel, O. Milton, M. A. Mostrom, D. A. Muirhead, T. D. Mulville, J. J. Ramirez, L. E. Ramirez, and T. M. Romero, "Flashover of a vacuum-insulator interface: A statistical model," *Phys. Rev. ST Accel. Beams*, vol. 7, no. 7, p. 070401, July2004.

[6] O. Milton, "Pulsed Flashover of Insulators in Vacuum," *Electrical Insulation, IEEE Transactions on [see also Dielectrics and Electrical Insulation, IEEE Transactions on]*, vol. 7, no. 1, pp. 9-15, Mar.1972.

[7] A. Watson, "Pulsed Flashover in Vacuum," *Journal of Applied Physics*, vol. 38, no. 5, pp. 2019-2023, Apr.1967.

[8] W. A. Stygar, R. B. Spielman, G. O. Allshouse, C. Deeney, D. R. Humphreys, H. C. Ives, F. W. Long, T. H. Martin, M. K. Matzen, D. H. McDaniel, C. W. Mendel, Jr., L. P. Mix, T. J. Nash, J. W. Poukey, J. J. Ramirez, T. W. L. Sanford, J. F.

Seamen, D. B. Seidel, J. W. Smith, D. M. Van De Valde, R. W. Wavrik, P. A. Corcoran, J. W. Douglas, I. D. Smith, M. A. Mostrom, K. W. Struve, T. P. Hughes, R. E. Clark, R. W. Shoup, T. C. Wagoner, T. L. Gilliland, and B. P. Peyton, "Design and performance of the Z magnetically-insulated transmission lines,", 1 ed 1997, pp. 591-596.

[9] H. C. Miller, "Surface flashover of insulators," *Electrical Insulation, IEEE Transactions on [see also Dielectrics and Electrical Insulation, IEEE Transactions on]*, vol. 24, no. 5, pp. 765-786, 1989.

[10] J. M. Elizondo, T. H. Martin, K. W. Struve, and L. F. Bennett, "The Z-20 reliability calculations,", 2 ed 2003, pp. 895-898.

[11] VanDevender J.P., "Vacuum Insulators and Magnetically Insulated Power Flow," Air Force Aero Propulsion Laboratory,Pulsed Power Lecture Series # 19, 1982.

[12] C. L. Enloe, "The equilibrium charge distribution and electric field at a vacuum/dielectric interface," *Journal of Applied Physics*, vol. 65, no. 9, pp. 3329-3334, May1989.

[13] Ansoft, "Maxwell SV," Ansoft, 2006.

[14] Boersch H., Hamish H., and Ehrlich W., "Surface Discharges Over Insualtors in Vacuum," *Z. Angew. Phys.*, vol. 15, pp. 518-525, 1963.

[15] J. M. Elizondo, M. L. Krogh, D. Smith, D. Stoltz, S. N. Wright, S. E. Sampayan, G. J. Caporaso, P. Vitello, and N. Tishchenko, "Vacuum surface flashover and high pressure gas streamers,", 2 ed 1997, pp. 1027-1032.

[16] A. S. Pillai and R. Hackam, "Influence of metal-insulator junction on surface flashover in vacuum," *Journal of Applied Physics*, vol. 61, no. 11, pp. 4992-4999, June1987.
0

[17] R. A. Anderson, "Anode-Initiated Surface Flashover," 1979, pp. 173-179.

[18] V. A. Nevrovsky, "Analysis of elementary processes leading to surface flashover in vacuum,", 1 ed 1998, pp. 159-161.

[19] K. D. Bergeron, "Theory of the secondary electron avalanche at electrically stressed insulator-vacuum interfaces," *Journal of Applied Physics*, vol. 48, no. 7, pp. 3073-3080, July1977.

[20] C. H. De Tourreil and K. D. Srivastava, "Mechanism of Surface Charging of High-Voltage Insulators in Vacuum," *Electrical Insulation, IEEE Transactions on [see also Dielectrics and Electrical Insulation, IEEE Transactions on]*, vol. EI-8, no. 1, pp. 17-21, 1973.

[21] R. A. Anderson and J. P. Brainard, "Mechanism of pulsed surface flashover involving electron-stimulated desorption," *Journal of Applied Physics*, vol. 51, no. 3, pp. 1414-1421, Mar.1980.

[22] J. P. Vigouroux, O. Lee-Deacon, C. Le Gressus, C. Juret, and C. Boiziau, "Surface Processes Occurring during Breakdown of High-Voltage Devices," *Electrical Insulation, IEEE Transactions on [see also Dielectrics and Electrical Insulation, IEEE Transactions on]*, vol. EI-18, no. 3, pp. 287-291, 1983.

[23] M. E. Savage, W. A. Stygar, J. M. Elizondo, H. C. Ives, W. Shoup, K. W. Struve, and D. H. McDaniel, "Effect of self-magnetic field on large pulsed insulators operated at 4 megavolts and 5 megaamperes," 2004, pp. 54-59.

[24] J. P. VanDevender, D. H. McDaniel, E. L. Neau, R. E. Mattis, and K. D. Bergeron, "Magnetic inhibition of insulator flashover," *Journal of Applied Physics*, vol. 53, no. 6, pp. 4441-4447, June1982.

[25] J. Golden and C. A. Kapetanakos, "Flashover breakdown of an insulator in vacuum by a voltage impulse in the presence of a magnetic field," *Journal of Applied Physics*, vol. 48, no. 4, pp. 1756-1758, Apr.1977.

[26] M. Lehr, R. Korzekwa, H. Krompholz, and M. Kristiansen, "Magnetic-field effects on vacuum insulator flashover," *Journal of Applied Physics*, vol. 71, no. 1, pp. 389-394, Jan.1992.

[27] K. D. Bergeron and D. H. McDaniel, "Magnetic inhibition of surface flashover of insulators in vacuum," *Applied Physics Letters*, vol. 29, no. 9, pp. 534-536, Nov.1976.

[28] K. R. LeChien, J. M. Gahl, M. A. Kemp, R. D. Curry, J. M. Elizondo, and K. W. Struve, "Development of a terawatt test stand at the University of Missouri for fast, multichannel switching analysis,", 2 ed 2003, pp. 1051-1053.

[29] D. L. Johnson, "Initial Proto II Pulsed Power Tests," 1976.

[30] K. R. LeChien, "Implementation of the University of Missouri Terawatt Test Stand and the Study of a Large, Multichanneling, Laser Triggered Spark Gap." 2006.

[31] C.R.Hicks and K.V.Turner Jr., *Fundamental Concepts in the Design of Experiments*, 5 ed Oxford University Press Inc., 1999.

[32] "Statistical Analysis Software (SAS)," 2007.

[33] "Statistical Analysis Software (SAS)," 2007.

[34] M.J.Kiemele, S.R.Schmidt, and R.J.Berdine, *Basic Statistics*, 4 ed Oxford University Press Inc., 1999.